國 立 交 通 大 學

電信工程研究所

碩 士 論 文

利用一維電磁帶隙結構設計之
五頻近地印刷型單極天線

A Printed Penta-band Ground-Proximity

Monopole Antenna Designed Using

One-Dimensional EBG Structures

研 究 生：楊子嫺　　　(Tzu-Hsien Yang)

指導教授：鍾世忠 教授　(Dr. Shyh-Jong Chung)

中 華 民 國 九 十 九 年 七 月

利用一維電磁帶隙結構設計之
五頻近地印刷型單極天線

A Printed Penta-band Ground-Proximity Monopole Antenna

Designed Using One-Dimensional EBG Structures

研 究 生：楊子嫻　　　　Student : Tzu-Hsien Yang

指導教授：鍾世忠 博士　　Advisor : Dr. Shyh-Jong Chung

國立交通大學

電信工程研究所

碩士論文

A Thesis

中 華 民 國 九 十 九 年 七 月

利用一維電磁帶隙結構設計之
五頻近地印刷型單極天線

研究生：楊子嫻　　　　　指導教授：鍾世忠 博士

國立交通大學電信工程研究所

碩士論文

摘要

　　隨著筆電無線通訊的發展，運用於筆電的內嵌式五頻天線的需求逐漸增長。在筆電內嵌式天線運用中，天線的寬度被筆電邊緣寬度所限制，所以需要一個近地且狹小的天線設計。然而，當天線非常接近地平面時，因為受到地面反向鏡像電流的影響，天線的效率勢必會減少。為了解決這個問題，我們將電磁能隙結構運用於地面邊緣處，如此可以改善接地面鏡像電流所造成的阻抗匹配、天線增益退化等問題，因此可將天線直接放置於具有高阻抗電磁表面的金屬接地面之上，而不影響原有天線特性。

　　本論文提出一種一維電磁能隙結構，不同於傳統的電磁帶隙結構，此一維電磁能隙結構採用印刷方式實現並聯 LC 共振電路，能有效縮小結構體積並有利於簡單製作。根據上述優勢，本論文提出兩種利用一維電磁能隙結構所設計的平面印刷近地天線，此兩種天線皆可用低成本的 FR4 基板製造。首先提出一個利用一維電磁能隙結構設計之高效率近地偶極天線，該天線與地面之間的距離只有 10 毫米，整體尺寸 10 毫米×153 毫米。此天線擁有良好的效能，量測的天線輻射效率在 GSM（824 MHz-960 MHz）頻段中皆有 55.6%以上。接著提出一個利用一維電磁能隙結構設計之五頻（GSM850/900/1800/1900/UMTS）近地單極天線。在此我們結合兩種不同的一維電磁能隙結構來提供較寬的電磁能隙結構共振頻寬，如此一來可以將

單極天線近地放置且在 GSM (824 MHz-960 MHz)頻段中仍維持良好的天線效能。在較高的頻段(1710 MHz-2170 MHz)中，一部份的一維電磁能隙結構能夠產生新的電流路徑並有效的輻射，達成五頻天線的需求。相較於之前的設計，第二個天線擁有較小的尺寸和更大的頻寬。此天線尺寸為 10 毫米×63 毫米，且在五頻頻段中皆有超過 51.5%的輻射效能。鑑於此一維電磁能隙結構擁有縮小的面積和良好的設計的靈活性，因此很適合運用於近地印刷式天線設計，以符合商業天線應用。

A Printed Penta-band Ground-Proximity Monopole Antenna Designed Using One-Dimensional EBG Structures

Student : Tzu-Hsien Yang   Advisor : Dr. Shyh-Jong Chung

Institute of Communication Engineering

National Chiao Tung University

ABSTRACT

The demand for compact internal WWAN (Wireless Wide Area Network) antenna embedded in the laptop computer for penta-band operation has seen growing attention. For laptop computer applications, the width of the antenna is limited to the overall width of the edge of laptop computers, which results in narrow and low profile needs. However, when the antenna is very close to the ground plane, it is bound to reduce the antenna efficiency. To solve this problem, the EBG structure is applied to the ground plane, which behaves as a high impedance surface at the resonance frequency of the EBG structure. Thus, the antenna can placed close to the ground plane while maintaining the antenna performance.

The new 1-D EBG structure is proposed in this thesis. Unlike the conventional EBG structures, the proposed 1-D EBG structure utilizes a printed parallel LC circuit, which is more compact and easy to fabricate. According to the advantages shown above, two antenna applications base on the 1-D EBG structure are presented. Both of them are fabricated on low cost FR4 substrate of 0.4 mm. First, a high efficiency ground-proximity dipole antenna using 1-D EBG structure is designed. The distance between antenna and the ground plane is only 10 mm with the overall size of 10 mm $\times$ 163 mm. The good radiation properties are obtained with the measured radiation efficiency over 55.6% for GSM (824 MHz-960 MHz) applications.

Secondly, the penta-band (GSM850/900/1800/1900/UMTS) ground-proximity printed penta-band monopole antenna is achieved with different 1-D EBG structures combined together. These 1-D EBG structures are combined to provide wider EBG operation bandwidth for GSM (824 MHz-960 MHz), so the monopole antenna and ground plane can be placed in close proximity without affecting the antenna performance in the lower band. In the higher band (1710 MHz-2170 MHz), the 1-D EBG structures can be viewed as efficient radiators, which create additional two resonances and penta-band is thus achieved. Compared to the previous design, the second antenna has a smaller size of 10 mm × 63 mm. The radiation performance is still maintained, which is all above 51.5% in penta-band. Given the design flexibilities and compactness, the antenna designed with 1-D EBG structures is feasible to commercial applications.
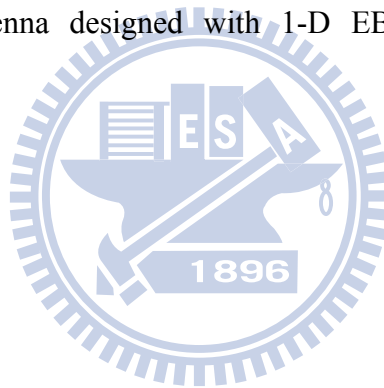
ACKNOWLEDGEMENT

在完成這篇碩士論文的同時，我首先要感謝的就是我的指導教授鍾世忠博士。從三年前開始做專題後，教授適時地給予指導，讓我逐漸熟悉天線的設計及原理，使我獲益良多，真的由衷感謝鍾世忠教授這三年來的指導。

在實驗室中，已經畢業的阿信學長在我還是專題生的時候教導我們許多基礎的概念；萬能的實驗室之母菁偉學姊，在研究上循序漸進的引導我們，一直很照顧著大家；凱哥學長教導我很多EBG的觀念，提供許多有創意的想法，甚至還會表演噴火呢！瘦瘦堂學長有問必答，最後還告訴我們許多口試的技巧，讓我順利的完成口試；羊羊學長是實驗室的棟樑，常常忙到很晚，但是還是很義氣的給予我們很好的意見和幫助；最後是助理珮華姐姐，處理包羅萬象的種種事件，很感謝你辛苦幫我們打理實驗室的大小事務，讓我們能無後顧之憂。感謝學長姐們和助理們的幫忙，我在這三年裡我收穫匪淺。

跟我同屆的碩二同學們，很開心可以跟你們一起畢業。同窗六年的冷肥，源源不絕的笑話和表演，感謝你對於炒熱實驗室的氣氛不遺餘力；一直跟我鬥嘴的財博，其實我知道你是刀子嘴豆腐心，感謝你在課業上的幫忙；總是在聊MSN的滿分逼逼，感謝你風雨無阻的帶我一起去校外量測，還分享許多笑料給大家；遠來求學的泰瑞莎，跟你聊天英文中文夾雜手語真的很有趣呢！實驗室的學弟們：溫馨幫大家慶生的志謙、天天裝水的瑋哥、愛打球的小豪、常常崩潰的老甘、常常看演唱會的阿澤，也很謝謝你們在這一年裡的幫忙。

最後我要特別感謝姵姵，在課業上或是生活上給予我很多的協助和包容，興趣相仿的我們能夠室友五年真的是緣份不淺。好友泡泡、Yuna夫婦、阿嬤、豪放等等，在交大六年你們一直是我的精神支柱！還有我親愛的家人們，無形的支持和關心也是我求學的最大動力。感謝這麼多人的幫忙讓我能順利的完成論文，在交大六年的生活非常充實愉快，謝謝大家！

CONTENTS

CONTENTS OF TABLES

CONTENTS OF FIGURES

Chapter 1 INTRODUCTION

1.1 BACKGROUND

The demand for compact internal WWAN (Wireless Wide Area Network) antenna which is embedded in the laptop computer covering penta-band operation is steadily growing [1]. This is a constant challenge for antenna designers, since higher degrees of global operation are sought, which, in turn, requires operation within continually more frequency. This is illustrated in Table I, which shows the nine bands allocated for the "3RD Generation"—or3G—UMTS Terrestrial Radio Access (UTRA) system. UTRA bands II, III, V, and VIII are also currently widely used by "2ND Generation"—or 2G—systems such as Global System for Mobile Communications (GSM). With the addition of UTRA band I, these bands allow quad-band 2G and tri-band 3G operation. Because of this, future laptop computer antennas are likely to be capable of operation in these bands, which are shown pictorially in Fig. 1.1 [2]. As indicated, bands II and V are used in the USA, whereas bands I, III, and VIII are used in Europe. All bands are also widely used worldwide, so designs of laptop computer antenna which covers the GSM850/900/1800/1900/UMTS operation frequency are required certainly.

TABLE I

UTRA FREQUENCY BANDS

Band	TX(MHz)	RX(MHz)
I	1920-1980	2110-2170
II	1850-1910	1930-1990
III	1710-1785	1805-1880
IV	1710-1755	2110-2155
V	824-849	869-894
VI	830-840	875-885
VII	2500-2570	2620-2690
VIII	880-915	925-960
IX	1749.9-1784.9	1844.9-1879.9
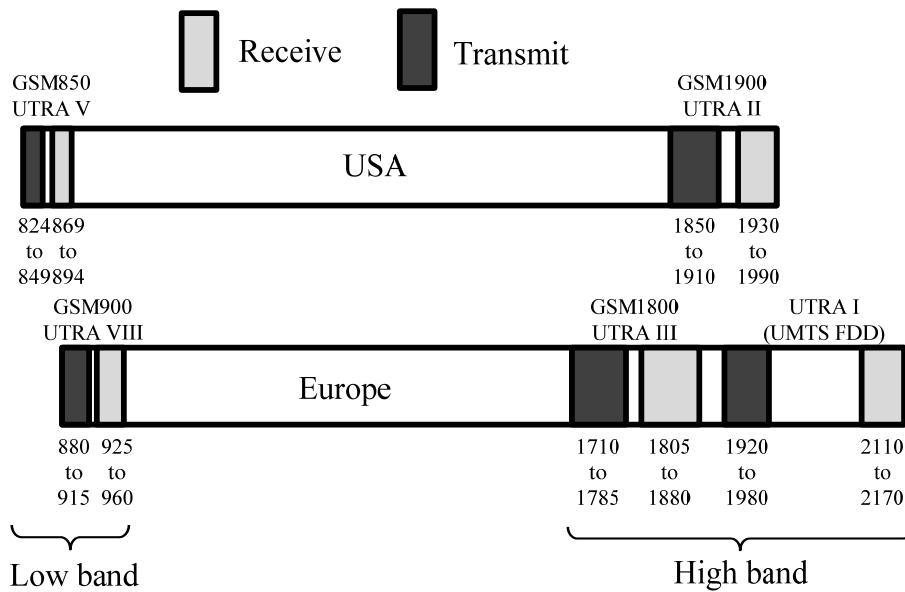
Figure 1.1: Common cellular frequency bands used in Europe and the USA (MHz).

And with the tendency of reducing size of laptop computers, the space of integrated antennas is limited to the edge of laptop computer's screen. When the conventional mobile communication antennas embedded in the laptop computers, it is difficult to achieve enough bandwidths or a larger antenna size is required for covering the penta-band operations. Therefore, by considering the thickness of laptop computers, printed antennas would be the proper radiating elements due to their low profile, small size and low weight, and their compatibility with planar surfaces. Furthermore, the width of antennas is mainly determined by the overall width of the edge of laptop computers, resulting in narrow and low profile needs. Nevertheless, when the antenna is very close to the ground plane, it is bound to be substantially eliminating current to reduce the antenna efficiency, thereby affecting the quality of communication.

In recent years achievements in improvement of the antennas' operational characteristics, by the utilization of electromagnetic band-gap (EBG) structures [3-19], have been reported. The EBG surfaces have a periodic pattern, and specific properties would be obtained by properly designing their lattice periodicity. They can be considered as a new type of conducting surface which can suppress propagating surface

wave if properly designed, and unlike normal conductors, the surface impedance is large and the EBG performs as a magnetic conductor. Therefore, if an antenna is located close to the EBG surface, its currents and their images are in phase and the theoretically expected phase inverse of the field does not occur when it is scattered by a usual metallic surface. This property permits a current source to be located very close to the EBG surface, without the fields produced by this and its image current is canceled, whereas enhancement of antenna gain is obtained. Thus, the EBG can function as a unique new type of ground plane for low-profile antennas with high directive gain, efficiency, and bandwidth.

In summary, discovery of EBG structures has revealed promising solutions to the above problems. In this thesis, a new type 1-dimentional EBG structure will be proposed and used to high efficiency ground-proximity antenna designs. And the interaction of antennas and 1-D EBG structures are extensively investigated.

1.2 LITERATURE SURVEY

EBG structures are usually realized by periodic arrangement of dielectric materials and metallic conductors. In general, they can be categorized into three groups according to their geometric configuration: (1) three-dimensional volumetric structures, (2) two-dimensional planar surfaces.

Figure 1.2 shows two representative 3-D EBG structures: a mushroom-like structure [20] and woodpile structure consisting of patches [21]. Examples of 2-D EBG surfaces are plotted in Fig. 1.3: a uni-planar design without vertical vias [22] and a planar dual-band EBG structure [23].

Top view

Top view

Cross view

Cross view

(a)

(b)
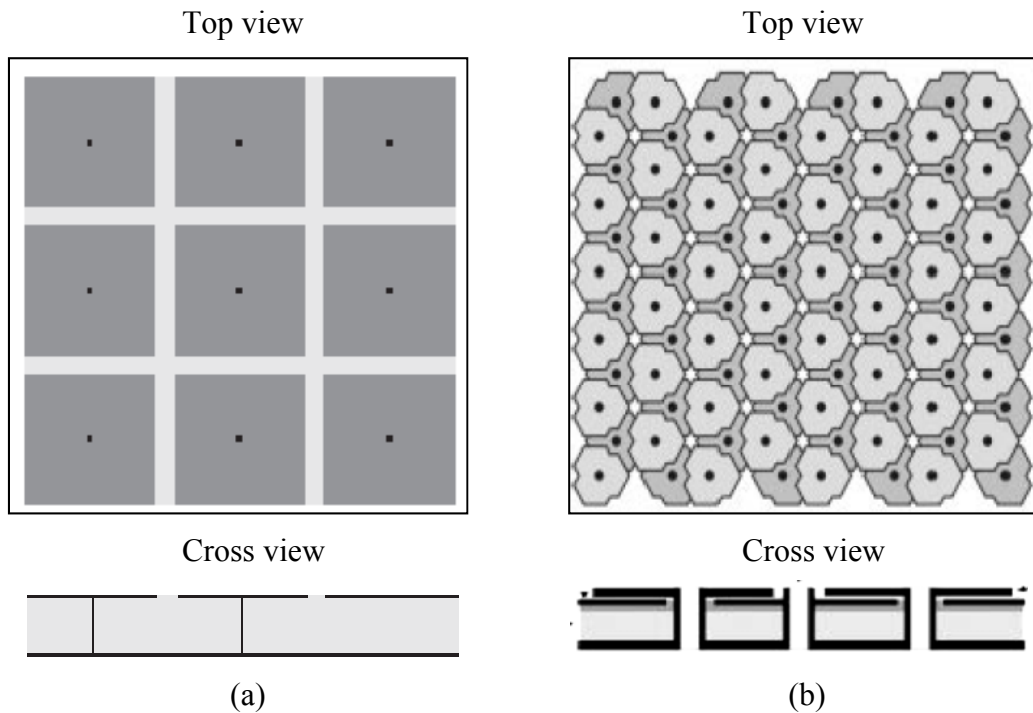
Figure 1.2: Three-dimensional EBG structures: (a) a mushroom-like structure and (b) a multi-layer metallic patch array.

Top view

Top view

Cross view

Cross view

(a)

(b)
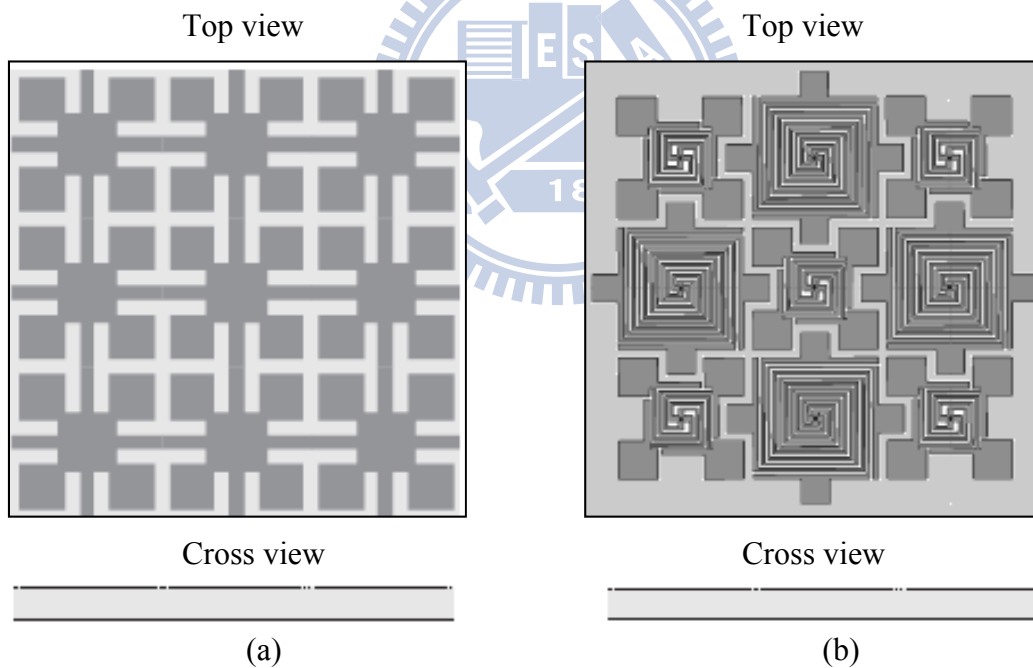
Figure 1.3: Two-dimensional EBG surfaces: (a) a uni-planar surface. (b) a dual-band EBG surfaces.

All of the mentioned EBG structures have similar operation characteristics, so we choose the most well known mushroom like 3-D EBG structure as an example, which is shown in Fig.1.2 (a). The structure consists of a periodic array of metal plates printed on a dielectric substrate, and each metal plate is connected to the ground plane using a

4
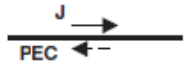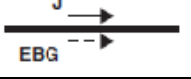
metal via. We defined L and C as the equivalent inductor and capacitor of a unit cell of the EBG structure, and the inductance of L depends on the thickness of the structure while the capacitance of C depends on the fringing electric fields between the pairs of metal plates. Thus the mushroom EBG structure forms a parallel LC circuit, and can be viewed as open circuit when this structure is operating at it's resonance frequency.

This interesting feature have led to a wide range of applications in antenna engineering, from wire antennas to microstrip antennas, and from the conventional antenna structures to novel surface wave antenna concepts and reconfigurable antenna designs. An application of EBG is to design low profile wire antennas with good radiation efficiency, which is desired in modern wireless communication systems. To illustrate the fundamental principle, Table II compares the EBG with the traditional PEC ground plane in wire antenna designs. When an electric current is vertical to a PEC ground plane, the image current has the same direction and reinforces the radiation from the original current. Thus, this antenna has good radiation efficiency, but suffers from relative large antenna height due to the vertical placement of the current. To realize a low profile configuration, one may position a wire antenna horizontally close to the ground plane. However, the problem is the poor radiation efficiency because the opposite image current cancels the radiation from the original current. In contrast, the EBG surface is capable of providing a constructive image current within a certain frequency band, resulting in good radiation efficiency.

Based on this concept, various wire antennas have been constructed on the EBG ground plane [24, 25]. For example, Fig. 1.4 shows a printed dipole antenna on mushroom like EBG structures. By optimizing the interaction between the impedances of a primary and image dipoles with the reflection phase of an EBG structure, a wideband printed dipole antenna was designed. In summary, the EBG surface exhibits a great potential for low profile efficient wire antenna applications.

TABLE **II**

COMPARISONS OF CONVENTIONAL PEC AND EBG GROUND PLANES IN WIRE ANTENNA DESIGNS

Options	Efficiency	Low profile
PEC	good	poor
PEC	poor	good
EBG	good	good
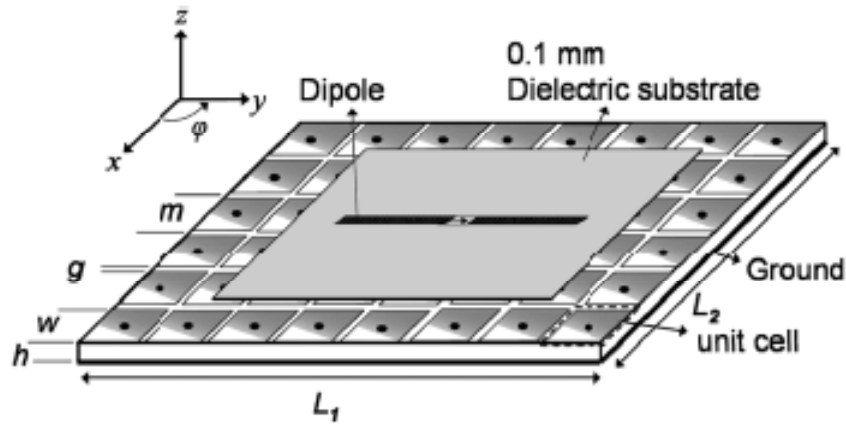
Figure 1.4: Low profile dipole antenna over a finite EBG ground plane

However, the conventional EBG must be periodic, which represents a large area. And when designed with the antenna, it will become a 3-D structure which is too large for today's wireless communication applications, so conventional EBG structures are lack of practicality.

1.3 CONTRIBUTION

To alleviate the above shortcomings of conventional EBG structures, this thesis presents a new type 1-D EBG structure, which both the antenna and EBG structure can be designed on the same plane to achieve an antenna in a limited narrow area in order to meet the needs of practical applications.

Fig. 1.5 shows the final design of printed ground-proximity monopole antenna with plane for penta-band operation in the laptop computer. The antenna was designed with proposed 1-D EBG structures which are printed on the two sides of substrate respectively, the gray parts represent the metal on the top side, and the dotted rectangle represents the metal on the other side. All relevant parameters and designing steps of the proposed antenna will be discussed in Chapter 4.

(a)

(b)
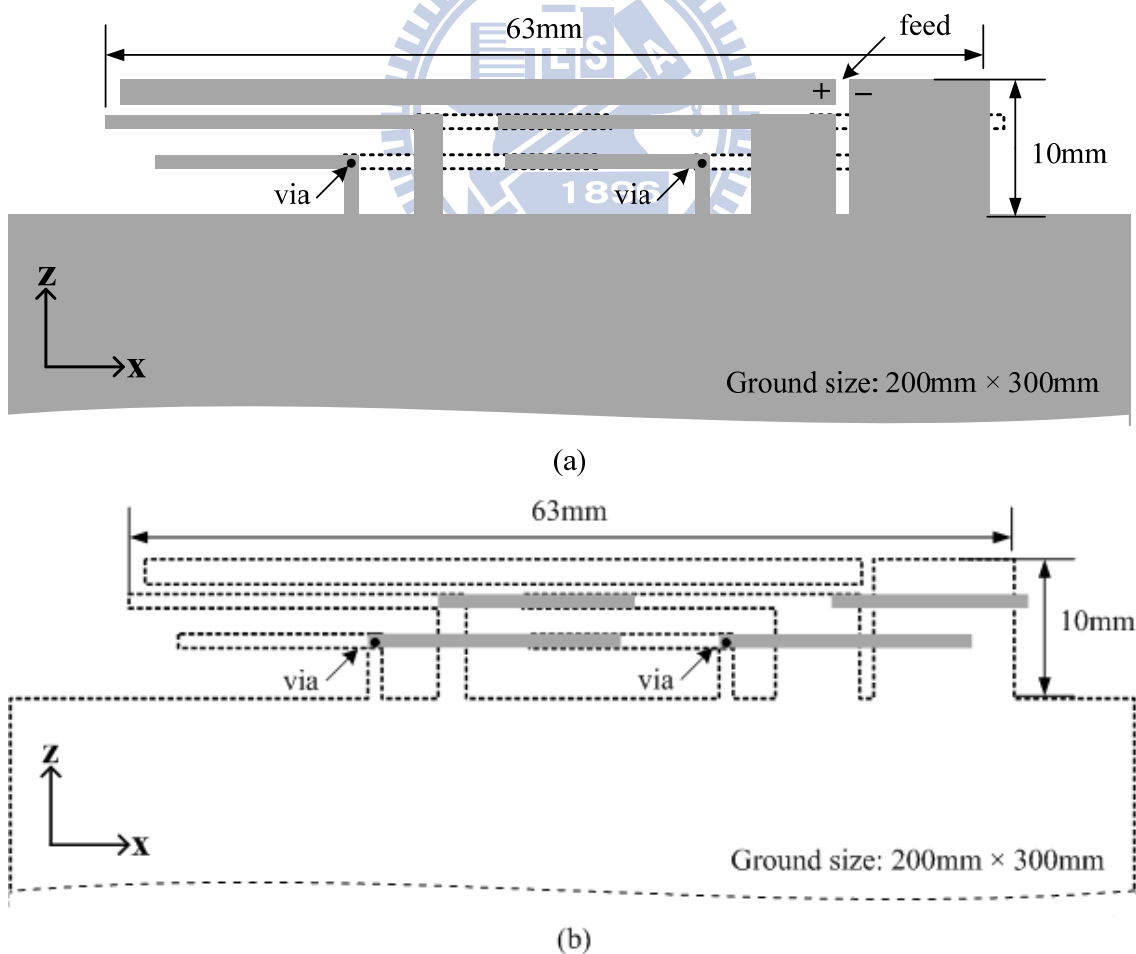
Figure 1.5: A printed ground-proximity penta-band monopole antenna designed with 1-D EBG structures. (a) Top view. (b)Bottom view.

In the proposed antenna, two different 1-D EBG structures were used to achieve enough GSM bandwidth (824~960MHz), and these 1-D EBG structures also can be viewed as new radiators at high frequencies, thus composed a penta-band antenna. The ground plane size is 200mm × 300mm while the total size of antenna is 10mm × 63mm, which means the proposed antenna occupies a reasonable volume and is suitable to be employed in the narrow space between the top edge of the display panel and the casing of the laptop computer. In summary, the proposed 1-D EBG structure can achieve a series of design requirements, such as low profile, compact size, broad bandwidth, and multiple functionalities, and be used for nowadays commercial applications.

1.4 THESIS ORGANIZATION

The thesis is organized as follows: Chapter 1 is an introduction, including the background, literature survey and contribution of proposed 1-D EBG structure. Chapter 2 presents the theory of EBG structures and shows the designing steps of the 1-D EBG structure. The simulation approaches and parameter investigations of the unit cell will also be shown in detail.

Chapter 3 depicts first application example of 1-D EBG structure, a high efficiency ground-proximity dipole antenna is proposed and used for GSM operation (824 MHz~ 960 MHz). The prototype is suitable to be embedded within a width of 10 mm between the top edges of the screen of a laptop and the antenna radiation efficiency is all above 55.6% in the using band.

Chapter 4 depicts a penta-band ground-proximity monopole antenna designed with 1-D EBG structures. Two different 1-D EBG structures are used in this antenna design to achieve enough GSM bandwidth. Also, the well designed 1-D EBG structures create new current paths at higher frequencies thus provide high bandwidth for

penta-band antenna. Furthermore, the total size of antenna is reduced and become more practical to commercial applications.

Finally, Chapter 5 concludes the overall thesis and also provides suggestions for the practical applications.

Chapter 2 ELECTROMAGNETIC BAND-GAP STRUCTURE DESIGN

This chapter is devoted to the designing process of conventional EBG and proposed 1-D EBG structure. The first section will depict the theory of EBG structures, and the unit cell characteristics will be described in detail. The second section will illustrate simulation approaches of EBG structures and the EM simulated results of proposed 1-D EBG structure will be shown.

A 1-D EBG structure will be designed in the end of this chapter, which will be applied to the GSM antenna (824 MHz-960 MHz) in next chapter. Also, the EM simulation method illustrated in this chapter will be used to design different 1-D EBG structures in Chapter 4.

2.1 THEORY OF ELECTROMAGNETIC BAND GAP (EBG) STRUCTURES

2.1.1 Theory of Conventional EBG Structure

When periodic structures interact with electromagnetic waves, characteristics such as frequency stop bands, pass bands, and band gaps could be identified. And periodic structures applications are seen in filter designs, gratings, frequency selective surfaces (FSS), photonic crystals and photonic band gaps (PBG), etc. We classify them under the broad terminology of "*Electromagnetic Band Gap (EBG)*" structures. Generally speaking, electromagnetic band gap structures are defined as artificial periodic (or sometimes non-periodic) objects that prevent/assist the propagation of electromagnetic waves in a specified band of frequency for all incident angles and all polarization states.

The EBG surfaces exhibit distinctive electromagnetic properties with respect to incident electromagnetic waves:

(1) When the incident wave is a surface wave ($k_x^2 + k_y^2 \leq k_0^2$, k_z is purely imaginary), the EBG structures show a frequency band gap through which the surface wave cannot propagate for any incident angles and polarization states. Atypical dispersion diagram is shown in Fig. 2.1(a).

(2) When the incident wave is a plane wave ($k_x^2 + k_y^2 \leq k_0^2$, k_z has a real value), the reflection phase of the EBG structures varies with frequency, as shown in Fig. 2.1(b). At a certain frequency the reflection phase is zero degrees, which resembles a perfect magnetic conductor that does not exist in nature.

In the above equations, k_x and k_y are the wavenumbers in the horizontal directions, k_z is the wavenumber in the vertical direction, and k0 is the free space wavenumber.

| (a) | (b) |
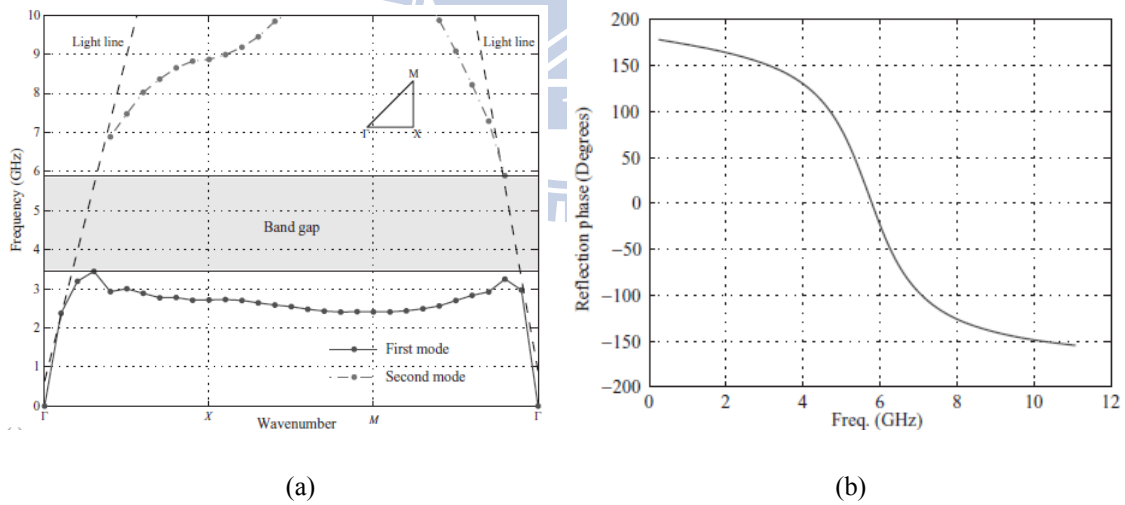
Figure 2.1: A planar EBG surface exhibits (a) a surface wave band gap and (b) an in-phase reflection coefficient for plane wave incidence.

Due to their unique band gap features, EBG structures can be regarded as a special type of metamaterial. Besides the band gap feature, EBG also possesses some other exciting properties, such as high impedance and PMC. For example, a mushroom-like EBG surface exhibits high surface impedances for both TE and TM polarizations. When

a plane wave illuminates the EBG surface, an in-phase reflection coefficient is obtained resembling an artificial magnetic conductor. These interesting features have led to a wide range of applications in antenna engineering.

2.1.2 Theory of 1-D EBG Structure

The unit cell of proposed 1-D EBG structure in shown in Fig.2.2 and is printed on the two sides of substrate respectively. The gray parts represent the metal on the top side, and the dotted rectangle represents the metal on bottom side, and both metals are connected by via. By considering the overlapping parts on the top and bottom sides, it can be seen as a parallel plate capacitor, which is circled by dotted line in Fig.2. And the current path through the via and the ground plane which is indicated by arrow line in Fig.2.2, provides an inductance. That is to say, when a plane waves transmits from + z axis towards −z axis, the equivalent circuit can be regarded as a parallel LC circuit. Both quantities form an equivalent parallel resonant circuit that describes the electromagnetic behavior of the material. Such structures perform as a high impedance surface around the specific frequency. Therefore, the metal ground plane can be regarded as PMC.
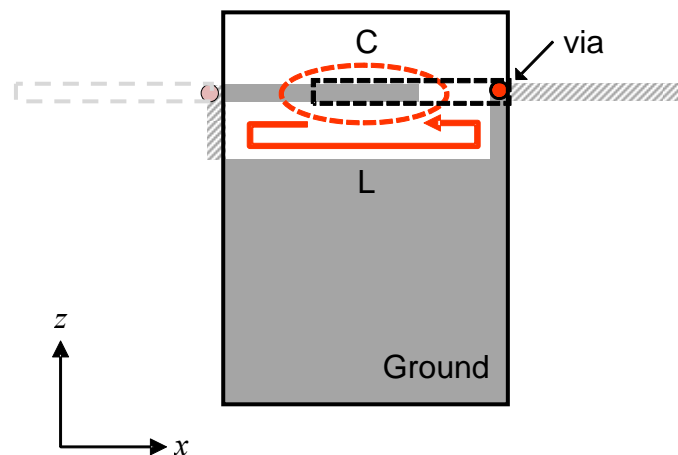
Figure 2.2: Unit cell of 1-D EBG structure. Dotted line circles parallel plate capacitor, and solid line elect current path through the via and the ground plane as an inductance.

2.2 SIMULATION APPROACHES TO EBG STRUCTURES

2.2.1 Simulation for Conventional EBG Structure

To analyze unique features of EBG structures, various methods have been implemented. These methods can be put into three categories: (1) periodic transmission line method, (2) lumped element model, and (3) full wave numerical methods.

The periodic transmission line method is another popularly used technique to analyze EBG structures [26]. Fig. 2.3 depicts a transmission line model of EBG structures, where Z_P is the impedance for each periodic element and X_C is the coupling capacitor. The Floquet periodic boundary condition is considered in this approach. After analyzing the cascaded transmission line, the dispersion curve can be readily obtained, which provides more information than the lumped element method. However, a difficulty in this method is how to accurately obtain the equivalent Z_P and X_C values for the EBG structures. So this method won't be used to design proposed 1-D EBG structure in this chapter.
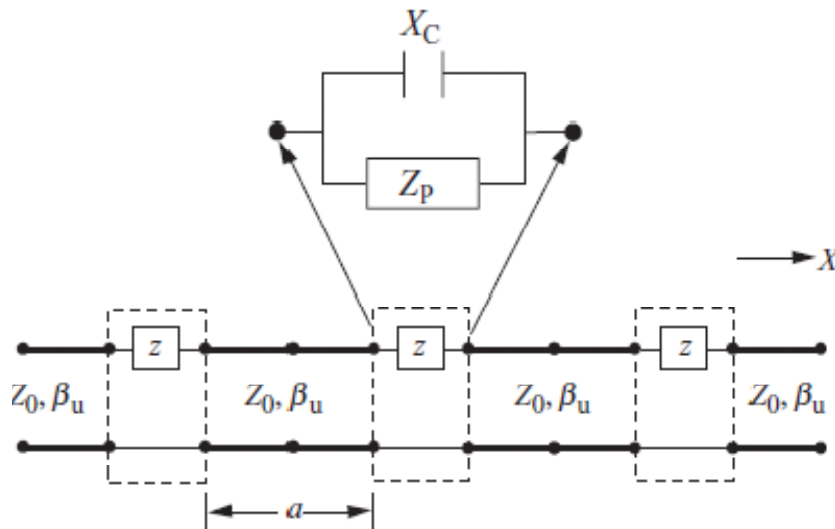
Figure 2.3: Periodic transmission line method for EBG analysis
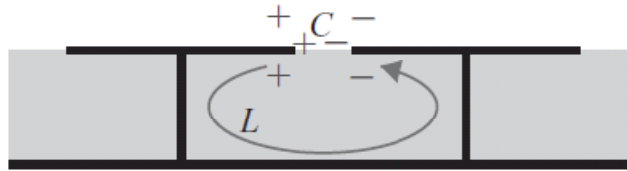
Figure 2.4: Lumped LC model for EBG analysis

The lumped element model is the simplest one that describes the EBG structure as an *LC* resonant circuit [27], as shown in Fig. 2.4. The values of the inductance *L* and capacitance *C* are determined by the EBG geometry and its resonance behavior is used to explain the band gap feature of the EBG structure. This model is simple to understand, but the results are not very accurate because of the simplified approximation of *L* and *C*.

Owing to the fast development in computational electromagnetic, various numerical methods have been applied in the full wave simulations of EBG structures. The advantage of the full wave numerical methods is the versatility and accuracy in analyzing different EBG geometries. For example, Fig. 2.5 depicts a model for the mushroom-like EBG analysis [28], and shows a unit cell model for the computation of the reflection phase at normal incidence.
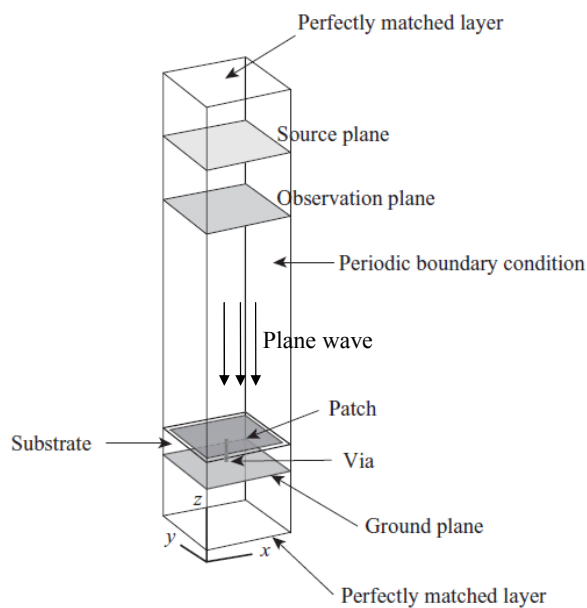
Figure 2.5: Full wave model of the EBG structure for reflection phase characterization.

In Fig. 2.5, a single unit cell is surrounded by perfectly matched layers (PML) along the z direction, which are positioned 0.55 λ above the EBG to absorb the reflected energy. And surrounding periodic boundary conditions (PBC) in the horizontal directions is set to model an infinite periodic structure. Because it is impossible to directly simulate infinite structure using limited computation resources, the computation domain needs to be truncated using proper boundary conditions. For this purpose, a PBC that models the effect of periodic replication is introduced to truncate the computational domain so that only a single unit cell needs to be simulated. The normally incident plane wave is launched on the top source plane, and an observation plane is set to record the reflected phase from the EBG surface, and the height of the observation plane is 0.50 λ.

It is observed in Fig. 2.1(b) that the reflection phase of the EBG surface decreases continuously from 180◦ to −180◦ as frequency increases. At low-frequency and high-frequency regions, the EBG surface shows a similar phase to a PEC case, which is 180◦ (or−180◦). At the frequencies the EBG surface exhibits a reflection phase close to 0◦, it resembles a PMC surface.

2.2.2 Simulation for 1-D EBG Structure

As the paragraph we mentioned previously, EBG surfaces are usually characterized through the evolution of the reflection phase over the frequency. To assess its reflection behavior, the structure is exposed to a plane wave, and the phase of the incident and the reflected waves are compared. In these cases, a single unit cell is modeled, and through the use of Periodic Boundary Conditions (PBCs) this cell is repeated infinitely.

By using Ansoft High Frequency Structure Simulator (HFSS) full-wave simulation software [29], simulation settings show in Fig. 2.6(a) (b). Fig. 2.6(a) is vertical top view of using four 1-D EBG unit cells toward -x direction, Fig. 2.6(b) is the side view of

A-A' cross-plane. The top side of Fig. 2.6 (a) is port1, and the bold line represent PEC plane, dotted line represent PMC plane. Because of the boundary conditions of PEC planes, the metal structures mirror and the unit cells repeat infinitely on the PEC sides. Whereas the boundary conditions of PMC plane assure the TEM surface wave. These settings are designed to fulfill periodic structure and plane wave feeding. It is important that the simulated result of Fig. 2.6 is identical to the simulated result of one unit cell. The reason for setting four unit cells instead of one is to confirm that the asymmetric unit cell can also be repeated periodically and infinitely by this EM simulation setting.
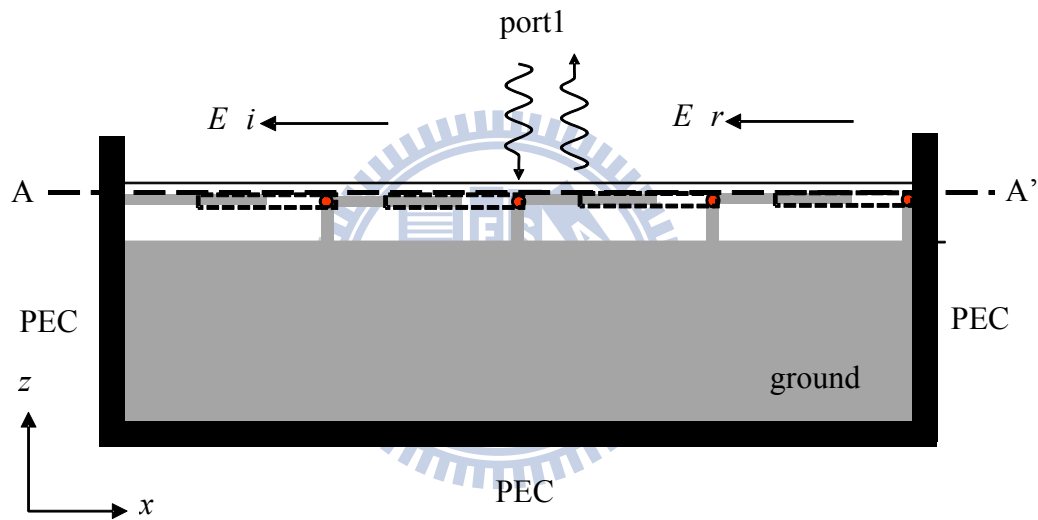
(a)
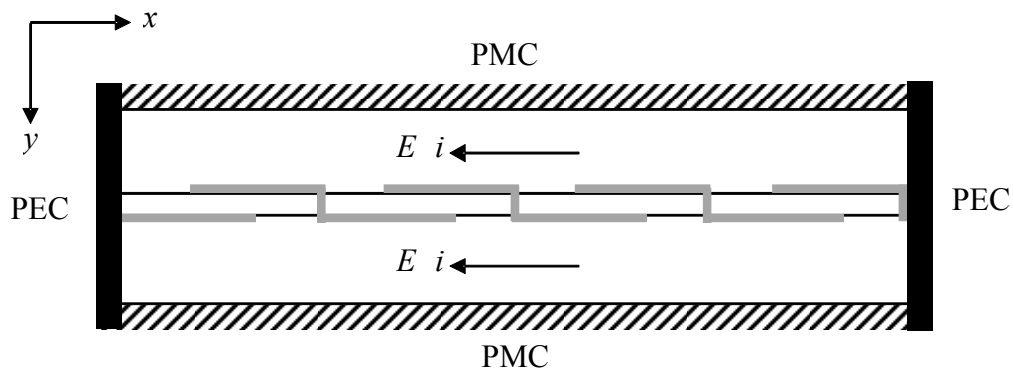
(b)

Figure 2.6: The settings of 1-D EBG structure simulation: (a) top view (b) A-A' side view.

In next chapter, we will design a GSM (824MHz- 960MHz) antenna as an application of 1-D EBG structure, so we choose 880MHz as the center frequency of the EBG structure in this section. The designed parameters of the unit cell is shown in Fig.2.7, where L_1 = 13.25 mm, L_2= 19 mm, H_1 = 4 mm, W_1 = 10 mm, W_2 = 1 mm, and the used substrate is FR4 with relative dielectric constant 4.4 and thickness of 0.4mm.
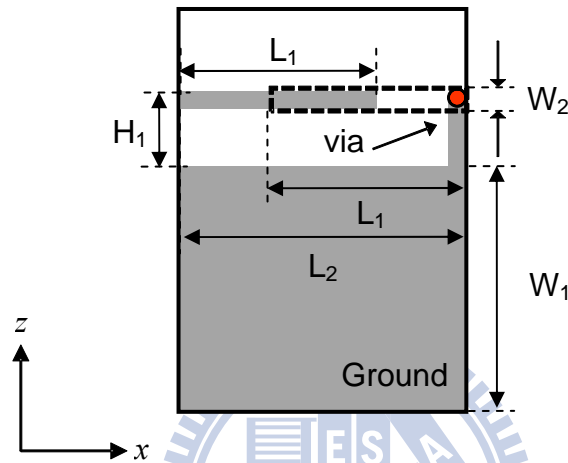
Figure 2.7: The parameter settings of the unit cell of 1-D EBG structure.

In general, when a plane wave incident into a PEC plane, the reflection phase will theoretically be 180 °, and when a plane wave incident into a PMC plane, the reflection phase will be 0 °. Fig. 2.8 shows the phase of S11 and frequency response of the proposed 1-D EBG structure. At resonant frequency 880 MHz, the reflection phase of A-A' plane equals to 0 °. This confirms that the structure is an EBG structure, thus can be regarded as a PMC plane.

The usable bandwidth of an EBG, when operating as a PMC plane, has been considered to be the frequencies over which the phase of the reflection coefficient is bounded by 90 degrees. The resonant frequency (fc) and fractional bandwidth (Fb) of 1-D EBG structure is given by formula (2.1) and (2.2):

$$f_c = \frac{\omega}{2\pi} = \frac{1}{2\pi\sqrt{LC}} \tag{2.1}$$

$$F_b = \frac{1}{R}\sqrt{\frac{L}{C}} \tag{2.2}$$

It is well known that this in-phase reflection bandwidth for a parallel LC circuit is proportional to $\sqrt{L/C}$, while the resonance frequency is proportional to $\sqrt{(1/LC)}$. Therefore, the in-phase reflection bandwidth increases due to the reduced C. And the increase in L for a specific resonance frequency has the added advantage of increasing bandwidth as smaller capacitance would be needed to achieve the same resonant frequency.
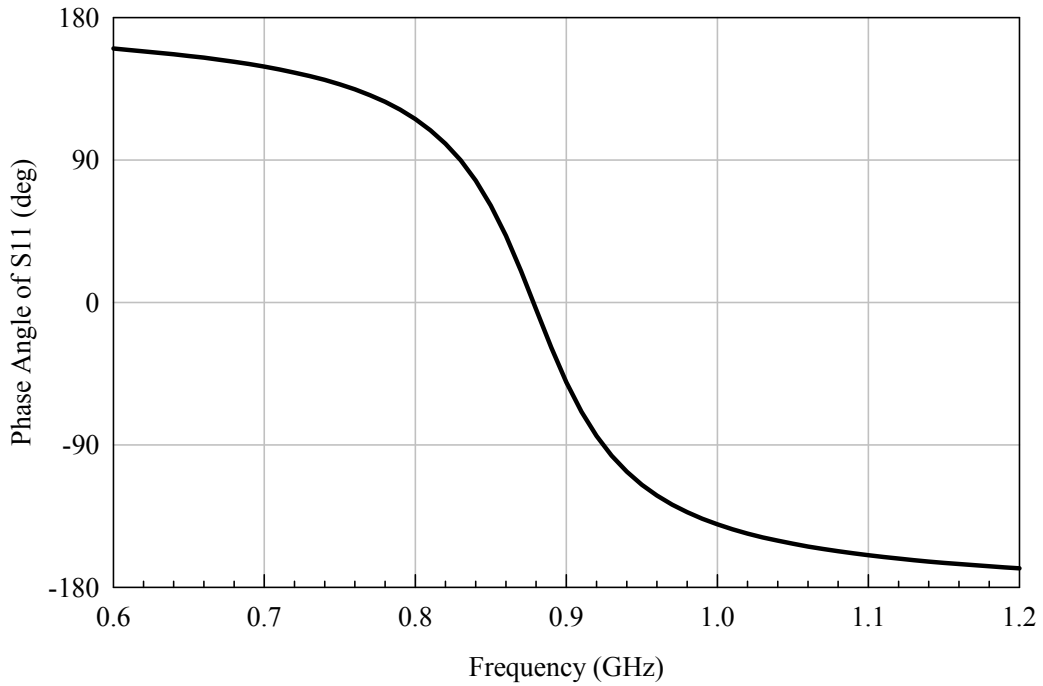
Figure 2.8: The reflection phase of 1-D EBG structure.

The resonant frequency of 1-D EBG structure can be designed by adjusting the length or width of the elements. Fig. 2.9 to Fig. 2.12 shows the changes in reflection phase while varying L_1, H_1, L_2, and W_2.

Fig. 2.9 shows that when L_1 varies from 12.25 mm to 14.25 mm, the center frequency moves from 970 MHz to 810 MHz and the bandwidth is decreasing. The resonant frequency is shifted downwards with increasing L_1, since the increasing L_1 will increase coupling capacitance while it does not affect the value of inductance. The increasing coupling capacitor also reduces the bandwidth of 1-D EBG structure. Fig. 2.10 shows that when H_1 varies from 3 mm to 5 mm, the center frequency moves from 938 MHz to 838 MHz and the bandwidth is increasing. The resonant frequency is also shifted downwards with increasing H_1, since the longer H_1 contributes to larger inductance while it does not affect the value of coupling capacitance. The lager inductance causes larger bandwidth, but also need more designing space. Fig. 2.11 shows that when L_2 varies from 17 mm to 21 mm, the center frequency moves from 860 MHz to 925 MHz and the bandwidth is increasing .The resonant frequency is shifted upwards with increasing L_2, since the increasing L_2 contributes to increasing value of inductance and decreasing value of coupling capacitance. Although longer L_2 will increase the unit cell size, the bandwidth of 1-D EBG can be improved effectively. Fig. 2.12 shows that when W_2 varies from 0.5 mm to 1.5 mm, the center frequency moves from 1100 MHz to 740 MHz and the bandwidth is decreasing. The resonant frequency is shifted downwards with increasing W_2. The increasing W_2 contributes to the increasing coupling capacitance while it does not affect the value of inductance. Also, lager coupling capacitance causes smaller bandwidth of 1-D EBG structure.

This simulation method yields good results when studying the theoretical behavior of the 1-D EBG surface, but does not assess real situations, in which the structure is always finite in size. For example, the characteristic properties of antennas are strongly influenced by the size of the ground plane, so it is therefore important to determine how the truncation of the infinite EBG cell distribution will affect the performance. The antenna applications of 1-D EBG structure will be proposed in Chapter 3 and Chapter 4.
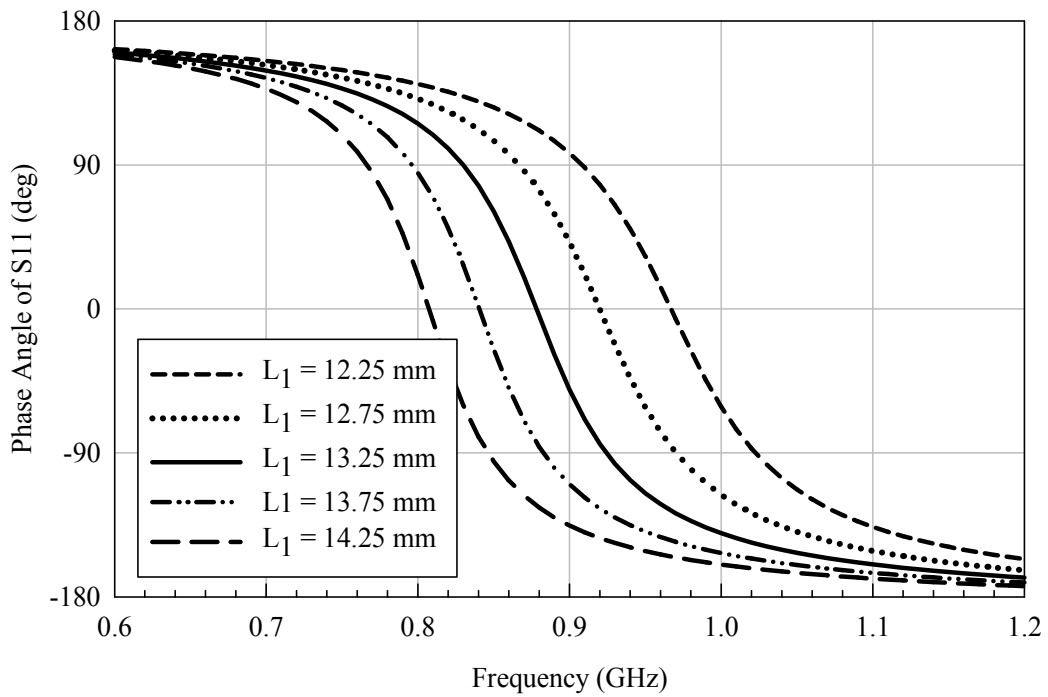
Figure 2.9: The reflection phase of 1-D EBG structure with H1 = 4mm, L2 = 19mm, W2=1mm and

varied L1 from 12.25 mm to 14.25 mm.
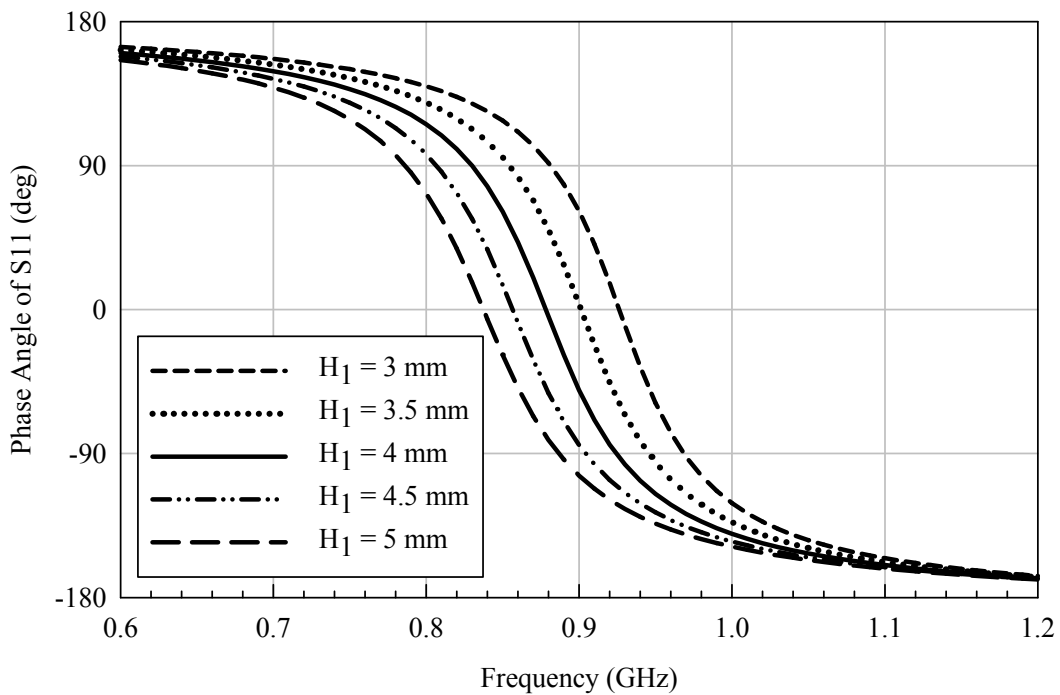
Figure 2.10: The reflection phase of 1-D EBG structure with L1 = 13.25mm, L2 = 19mm,

W2=1mm and varied H1 from 3 mm to 5 mm..
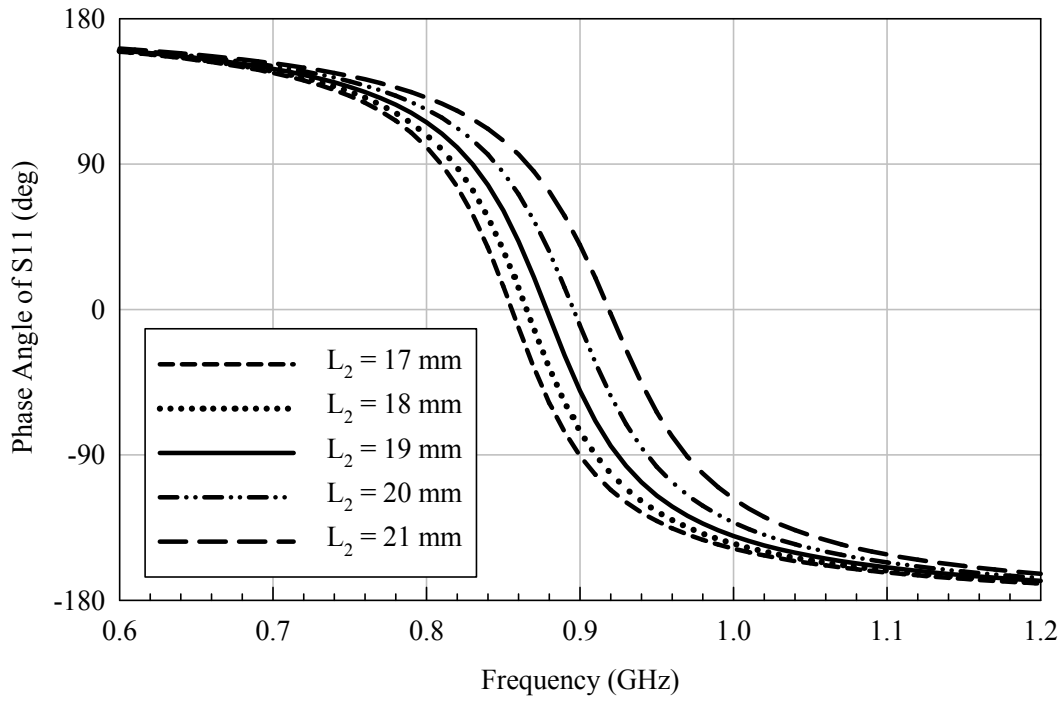
Figure 2.11: The reflection phase of 1-D EBG structure with H1 = 4mm, L1 = 13.25mm, W2=1mm and varied L2 from 17 mm to 21 mm.
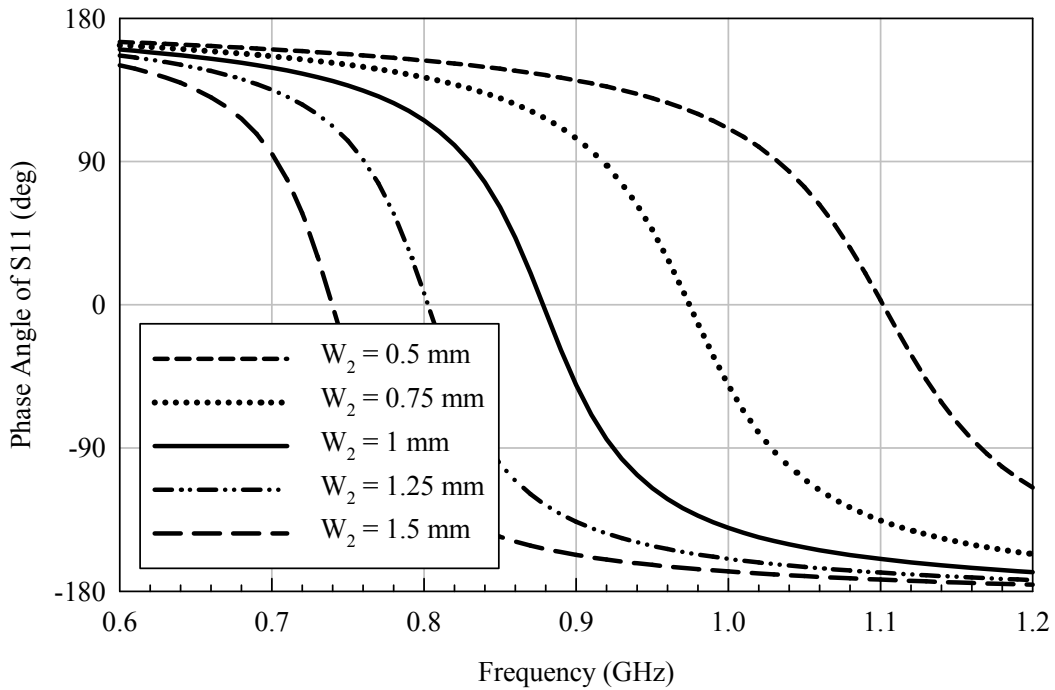
Figure 2.12: The reflection phase of 1-D EBG structure with H1 = 4mm, L1 = 13.25mm, L2=19mm and varied W2 from 0.5 mm to 1.5 mm.

Chapter 3 A HIGH EFFICIENCY GROUND-PROXIMITY DIPOLE ANTENNA

The 1-D EBG structure has been characterized and designed in previous chapter, and now we shift our focus to 1-D EBG applications in antenna engineering. The important property of 1-D EBG structures is the phase response to the plane wave illumination, where the reflection phase changes from 180∘ to −180∘ as the frequency increases. In this chapter, we utilize this property to improve the radiation efficiency of a dipole antenna near a ground plane.

The proposed antenna is shown in Fig. 3.1, we applied the 1-D EBG structure to the ground-proximity dipole antenna, thus the impedance matching and antenna gain degrade problem can be improved. Hence, the dipole antenna can be placed close to the high impedance surface of 1-D EBG structure on the ground plane and maintained the antenna performance. The used 1-D EBG structure will be shown briefly in section 3.1, design considerations of the dipole antenna with 1-D EBG structure are described in section 3.2, and measured results are presented in section 3.3.
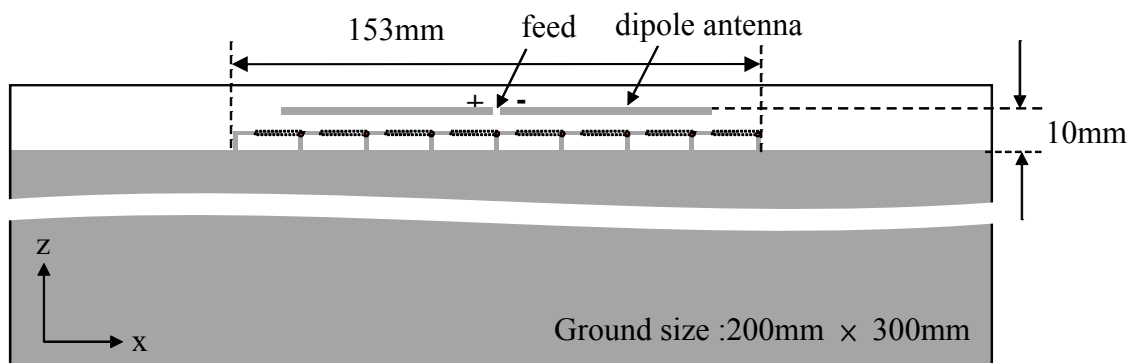
Figure 3.1: A high efficiency ground-proximity dipole antenna designed using 1-D EBG structure, and the total size of antenna is 10 mm ✕ 153 mm.

3.1 DESIGN OF 1-D EBG STRUCTURE

In this chapter, we use the 1-D EBG structure which was proposed in Chapter 2 and the unit cell parameters is shown in Fig. 3.2. The used substrate is FR4 with relative dielectric constant 4.4 and thickness of 0.4mm and the center frequency of this 1-D EBG structure is 880MHz.
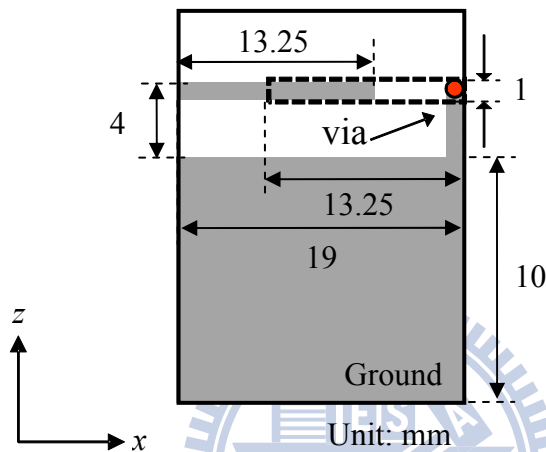
Figure 3.2: The parameters settings of the unit cell of 1-D EBG structure.

3.2 DESIGN OF A GROUND-PROXIMITY DIPOLE ANTENNA

Fig.3.1 is an application of 1-D EBG structure used in planar antenna design with a typical dipole antenna. We placed a designed dipole antenna next to the ground with 1-D EBG structure. The proposed antenna was designed for laptop computer application, so the ground size is 200 mm × 300 mm, which is used to simulate the upper ground plane of laptop computer.

The antenna is printed on the two sides of substrate respectively, the gray parts represent the metal on the top side, and the dotted rectangle represents the metal on the other side, and both metals of 1-D EBG structures are connected by via. Fig. 3.3 shows the related parameters of the antenna, where $L_1 = 13.25$ mm, $L_2 = 19$ mm, $L_3 = 61$ mm,

$H_1 = 4$ mm, $H_2 = 10$ mm. The length of dipole is used to tune the impedance match of the antenna. Therefore, the length of the dipole is not necessarily half-wavelength, and the simulated results show that a proper length is around 0.65λ for the proposed dipole antenna. Consequently, the total size of the proposed antenna is 10 mm $\times$ 153 mm.
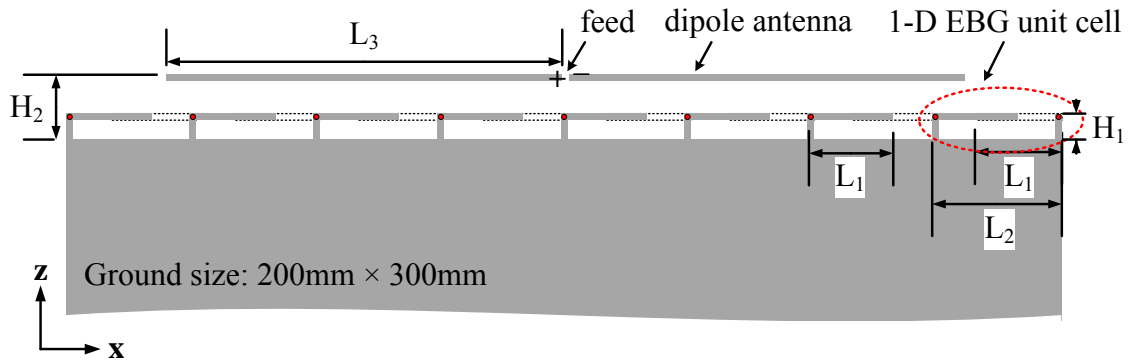
Figure 3.3: Parameters of the proposed antenna.

When the dipole antenna placed too close to a ground plane, the mirror current generated by the dipole antenna on the ground will be opposite to the current on the dipole antenna, which canceled each other. So both the impedance matching and radiation of the dipole antenna are destructed. However, when the edge of the ground added 1-D EBG structure, although the dipole antenna is very close to the ground plane, the antenna will still be able to maintain its original characteristics. This is because when a dipole is positioned on an EBG ground plane, no surface wave can be excited because of the surface wave band gap of the 1-D EBG structure. This phenomenon can be observed in current distribution diagram, which is shown in Fig. 3.4. The current distribution along the ground plane is weak at the resonance frequency of used 1-D EBG structure, that means the image current of the dipole antenna was suppressed by the 1-D EBG structure and the dipole antenna can radiate without being affected.
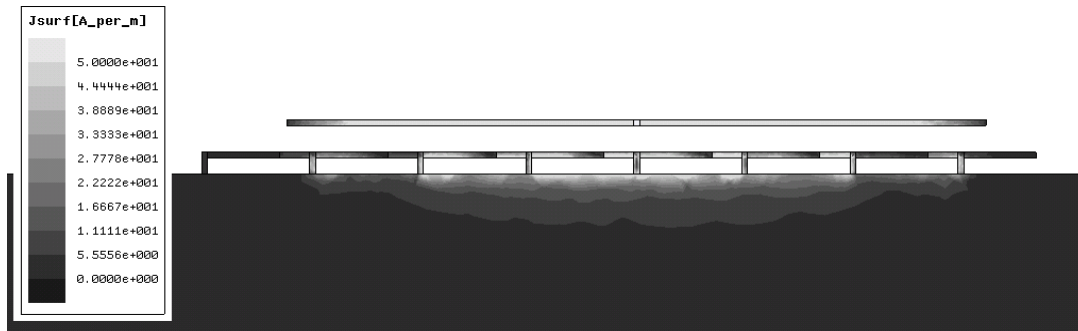
Figure 3.4: Current distributions of the dipole antenna with 1-D EBG structure at 880 MHz.

Fig. 3.5 shows the simulation results of return loss for original dipole antenna, dipole antenna with ground, and dipole antenna with 1-D EBG structure. In Fig. 3.5, the resonant frequencies are different between original dipole antenna and the dipole antenna with 1-D EBG structure. This is because when 1-D EBG structure was added, the far right and left unit cells of 1-D EBG structure will lead the equivalent length of antenna longer, and then cause the lower resonant frequency. Fig. 3.5 shows dipole antenna with 1-D EBG structure can achieve GSM bandwidth (824MHz~960MHz) ranges from 820MHz to 982MHz with a reflectivity of less than -6 dB.
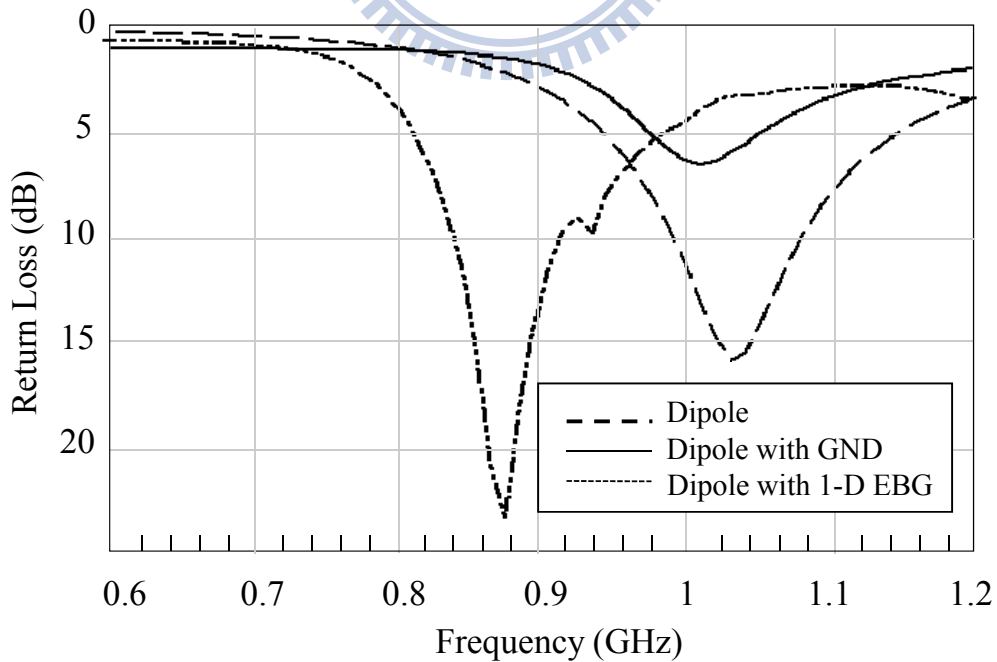
Figure 3.5: The simulated return loss of dipole antenna, dipole antenna with ground, and dipole antenna with 1D-EBG structure.

3.3 EXPERIMENTAL RESULTS

The realized proposed antenna is shown in Fig. 3.6.

Zoom in photo for antenna:

Ground size: 200mm × 300mm

(a)

Zoom in photo for antenna:

Ground size: 200mm × 300mm
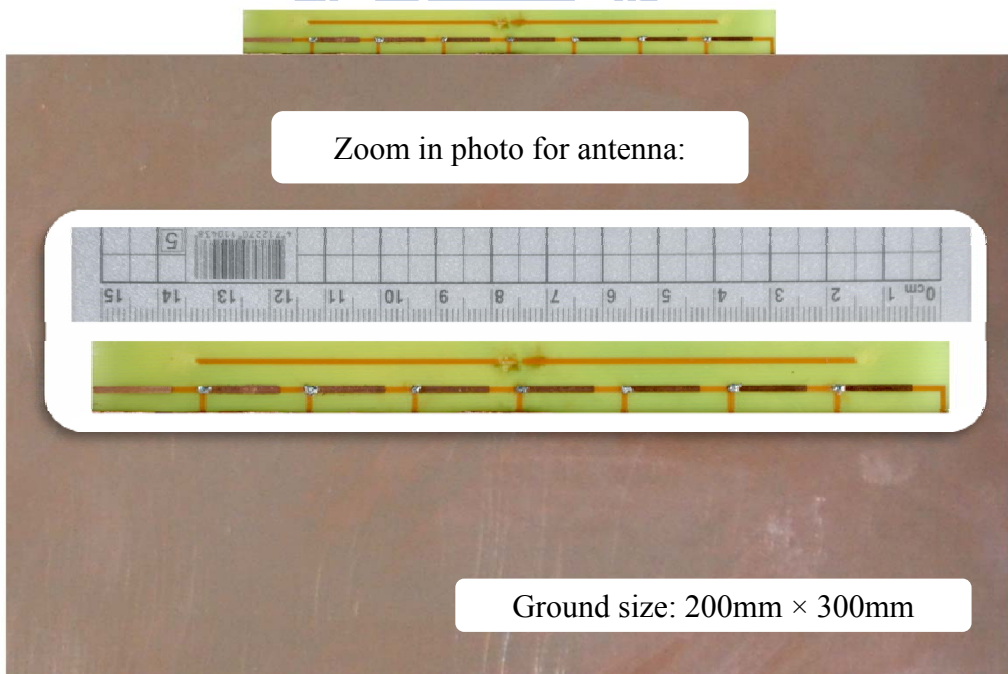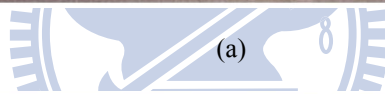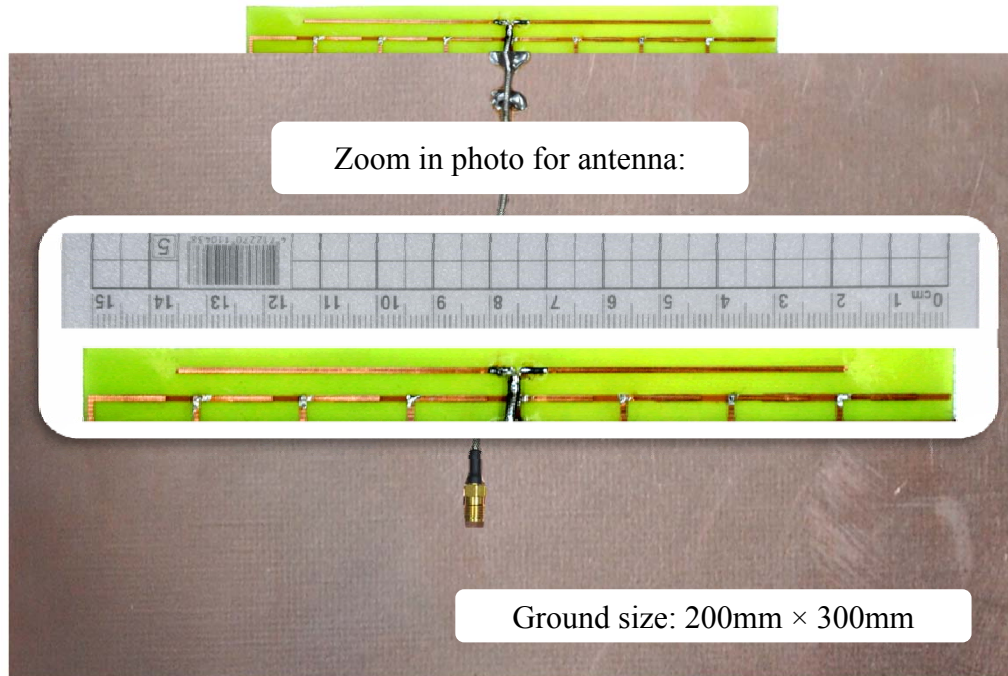
(b)

Figure 3.6: Photograph of the fabrication for the proposed antenna. (a) Top view. (b) Bottom view.

In Fig. 3.7, the dotted line represents the measured result and solid line represents the simulated result of dipole antenna with 1-D EBG structure. The measured bandwidth ranges from 802MHz to 968MHz with a reflectivity less than −6 dB, and the simulated and measured results come to a great agreement.
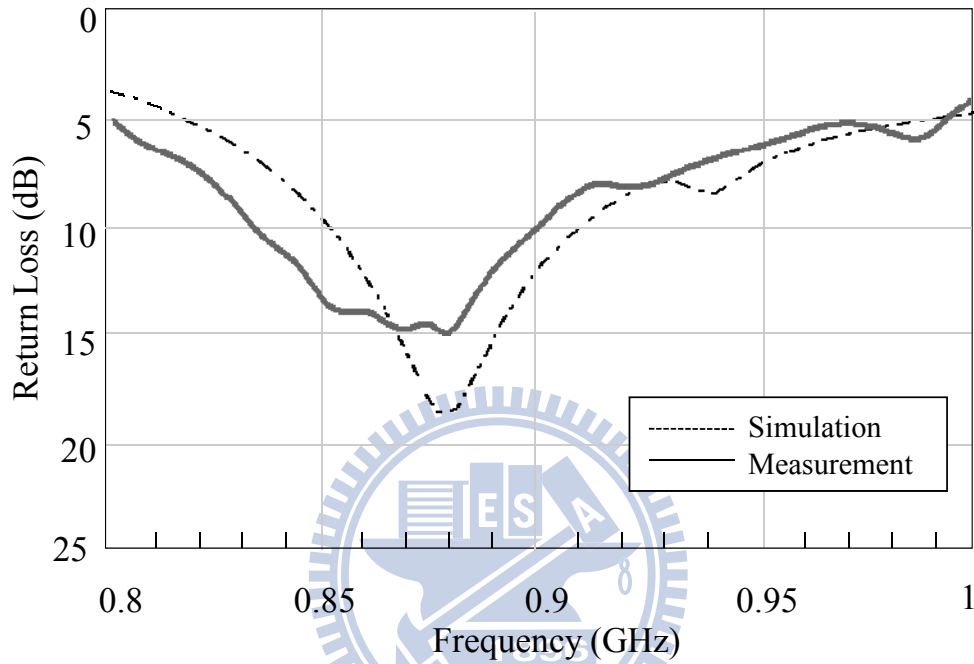
Figure 3.7: Simulated and measured results of dipole antenna with 1D-EBG structure.

Fig. 3.8 (b) depicts the measured and simulated radiation pattern of dipole antenna with ground in yz plane. In general, the radiation pattern of dipole antenna in this plane should be omnidirectional. However, the short distance between antenna and ground plane cause the mirror current on the ground plane opposite to the current on the antenna, and thus eliminate each other. This leads to skew radiation pattern. Fig. 3.8(a) is the measured and simulated radiation patterns of dipole antenna with 1-D EBG structure in *yz* plane. Compared Fig. 3.8 (a) to Fig. 3.8 (b), the radiation pattern becomes more identical to the radiation pattern of theoretical dipole antenna after adding 1-D EBG structure. This is because the mirror current on the ground is no longer reversed-phase when 1-D EBG structure is added. Therefore, 1-D EBG structure is able to improve the skewed pattern of the original problem.
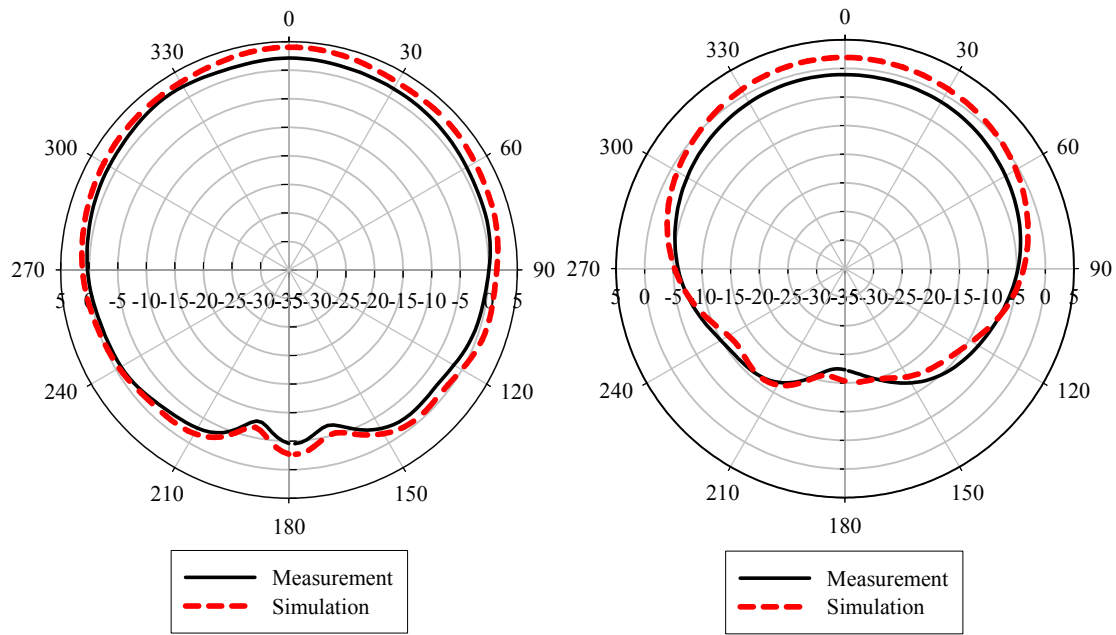
Figure 3.8: Radiation patterns in *yz* plane of (a) dipole antenna with 1-D EBG structure.

(b) Dipole antenna with ground..

In the design of traditional antennas which work in free space, the measured parameters are often the reflection coefficient S11 and the radiation patterns measured in the E or H planes around the antenna. The reflection coefficient describes how much of the available power is reflected at the antenna port, but it does not give any information about whether the remainder of the power is radiated or dissipated in the antenna. Therefore, the reflection coefficient alone cannot determine if the antenna is a good or a poor radiator. The efficiency is defined as being the total radiated power divided by the maximum available power when the antenna is impedance matched. The antenna efficiency includes the effects of mismatch, as well as absorption in the antenna and it's near field environment such as 1-D EBG structure.

As 1-D EBG structure absorbing part of the energy radiated from the antenna, efficiency becomes the key factor in the antenna design. Usually stronger ground current leads to higher energy losses, and moreover, less separation between them introduces stronger coupling effects. It is the in-phase reflection feature given by 1-D

EBG structure that effectively decreases the energy absorbed by the ground, thus improving the antenna efficiency.

Fig. 3.9 indicates the antenna efficiency in the given conditions: dipole antenna with ground and dipole antenna with 1-D EBG structure. As illustrated in those results, the dipole antenna with 1-D EBG structure has peak antenna efficiency 81.7% at 860MHz, when the dipole antenna is placed close to the ground without 1-D EBG structure, the antenna efficiency peak drops to 50.4% at 920MHz. In the bandwidth of GSM (824 MHz -960 MHz), the antenna efficiency of the dipole antenna with 1-D EBG structure are all above 55.6%, which has at least 10% enhancement to the case without 1-D EBG structure.
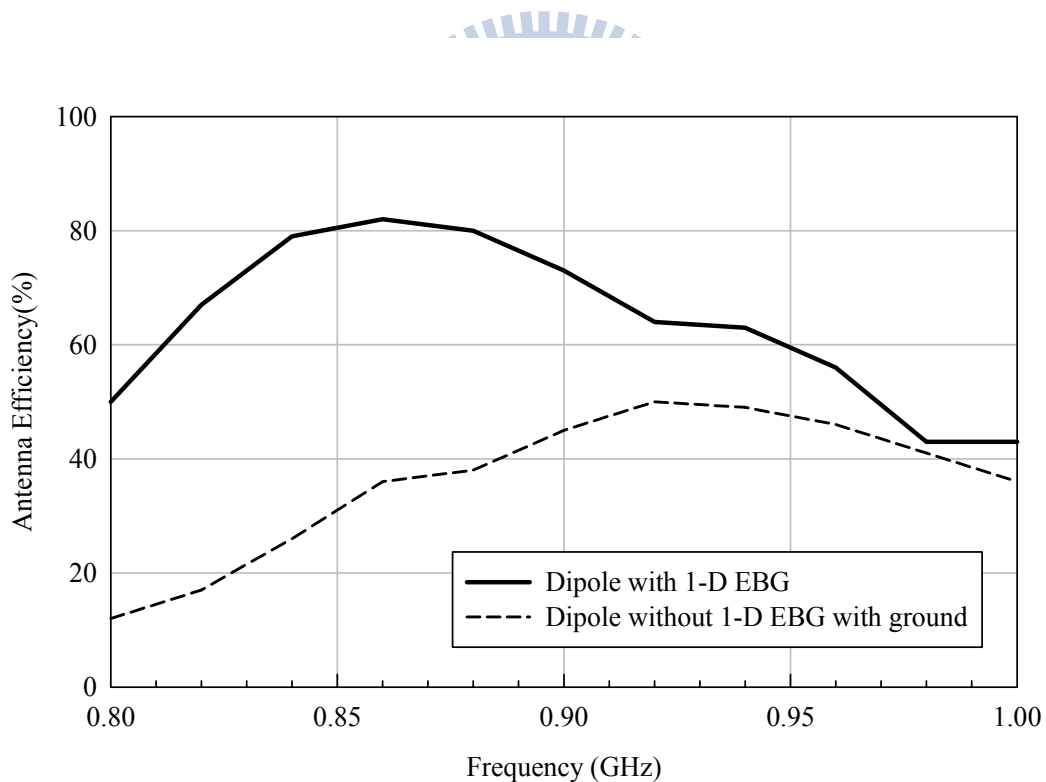
Figure 3.9: Antenna efficiency of dipole antenna with ground and dipole antenna with 1-D EBG structure.

Chapter 4 A PENTA-BAND GROUND-PROXIMITY MONOPOLE ANTENNA

In the previous chapter, a ground-proximity dipole antenna was proposed and the efficiency in GSM band has at least a 10% improvement by adding 1-D EBG structure. So we have confirmed that the 1-D EBG structure can shorten the necessary distance between antenna and ground plane, and allows antennas to maintain the original radiation characteristics. However, the total size of the dipole antenna proposed in Chapter 3 (10 mm $\times$ 153 mm) is still too large for commercial applications. Also the bandwidth only covers GSM band, which is not enough for WWAN antennas. Therefore, a more compact antenna with wider bandwidth is certainly demanded.

In this chapter, a penta-band ground-proximity monopole antenna is designed for laptop computer applications. Two 1-D EBG structures are applied to achieve low bandwidth while the structures can radiate in high band. In section 4.1, all design considerations and simulations of two new 1-D EBG structures will be illustrated. Those two 1-D EBG structures will be applied to ground-proximity monopole antennas respectively in section 4.2. Because either of the antenna does not have enough bandwidth for GSM operation, we combine those two 1-D EBG structures together in section 4.3. Furthermore, we adjusted part of the 1-D EBG structures slightly for impedance matching and create resonance at high frequencies, thus achieve penta-band requirement. And in the end of the section, an additional size reduction design will be proposed. The final design of the penta-band monopole antenna with proximate ground plane is shown in Fig. 4.1, and the total size of proposed antenna is 10 mm $\times$ 63 mm, which is more compact and applicable than the dipole antenna proposed in Chapter 3. The measured results are presented in section 4.4.
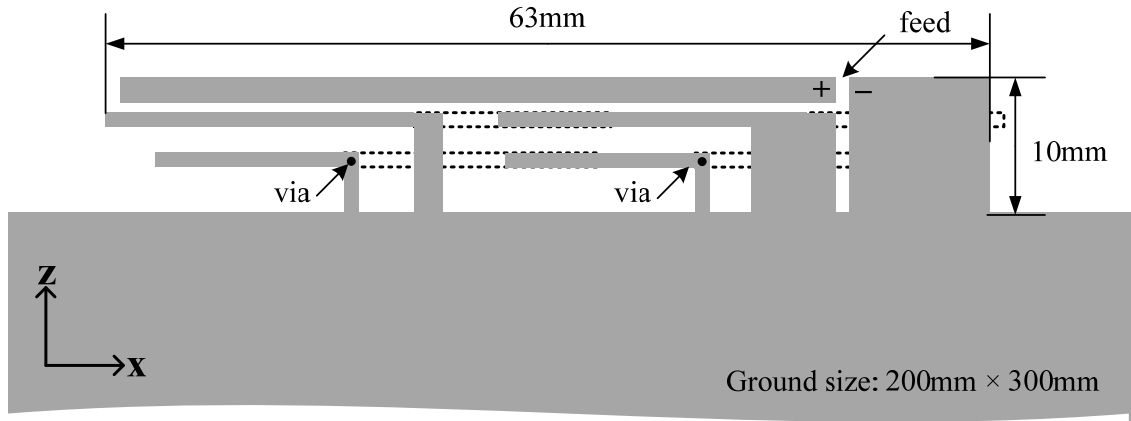
(a)
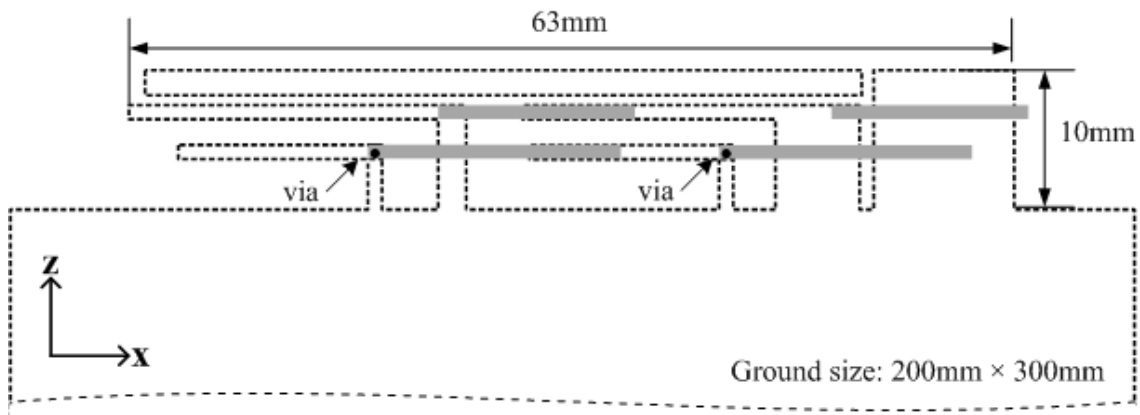
(b)

Figure 4.1: A printed penta-band ground-proximity monopole antenna designed using 1-D EBG structures.

(a) Top view. (b) Bottom view.

4.1 DESIGN OF 1-D EBG STRUCTURES

Two different 1- EBG structures are proposed in this section. The parameters of first 1-D EBG structure is shown in Fig.4.2, which is similar to the proposed structure in Chapter 3. This 1-D EBG structure can be viewed as parallel LC, and it is well known that the in-phase reflection bandwidth for a parallel LC circuit is proportional to $\sqrt{L/C}$, while the resonance frequency is proportional to $\sqrt{(1/LC)}$. So for certain resonance frequency, we fixed the total capacitance and inductance of the 1-D EBG structure, which means we varied L_2 and L_3 together with fixed H_2, L_4 and $L_2 + L_3$. Fig. 4.3 shows that the reflection phase will be the same when $L_2 = L_3 = 16.25$ mm and $L_2 = 14.5$ mm,

L_3 =18 mm with fixed L_4 = 25 mm and H_2=4.6 mm. The different combinations of L_2 and L_3 would be useful for impedance matching when we applied the 1-D EBG structure to antennas. The optimized parameters are L_2 = 14.5 mm, L_3= 18 mm, L_4= 25 mm, H_2 = 4.6 mm, W_3 = 1 mm, and the designed resonance frequency of first 1-D EBG structure is 840 MHz.
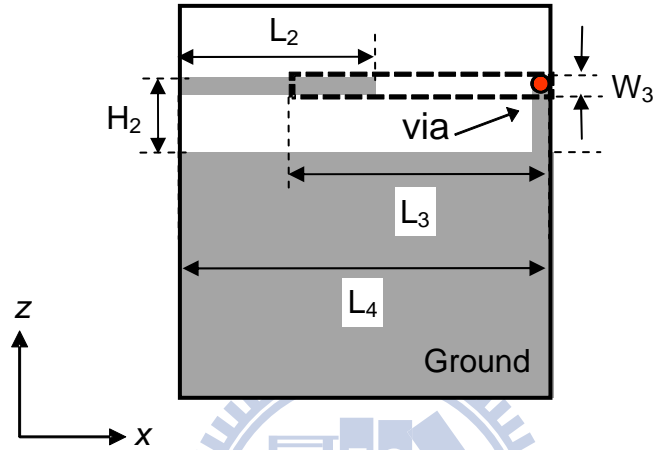
Figure 4.2: The unit cell of first 1-D EBG structure.
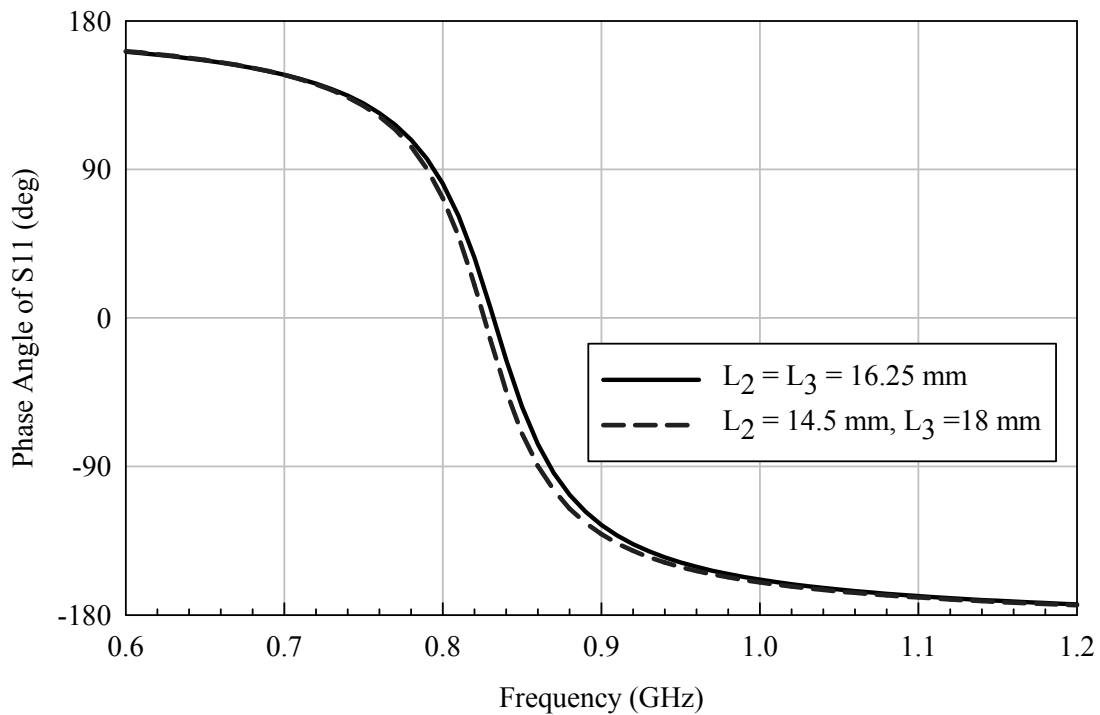
Figure 4.3: The reflection phase of first 1-D EBG structure with fixed L_4 = 25 mm and H_2= 4.6 mm.

The second 1-D EBG structure is shown in Fig. 4.5. The Fig. 4.5(a) depicts that the metal on the top right side of the unit cell can be viewed as a small monopole, which is equivalent to a shunt inductor (L). The microstrip line on the bottom left side couples to ground and forms a capacitor (Cground). And the overlapping parts on the top and bottom sides can be seen as a parallel plate capacitor (Ccoupling). In summary, the equivalent circuit of the structure is also a parallel LC circuit, which can form a 1-D EBG structure. The advantage of this 1-D EBG structure is easier to fabricate without using vias. Furthermore, it can be viewed as a monopole antenna at higher frequency if the impedance is matched well. However, more space is needed in this structure, because the second 1-D EBG structure needs longer microstrip line to achieve enough inductance without vias.

The optimized parameters of second 1-D EBG structure are illustrated in Fig 4.5(b), where $L_5 = 22$ mm, $L_6 = 14$ mm, $L_7 = 30$ mm, $H_3 = 7.8$ mm, $W_3 = 1$ mm, and the designed resonance frequency is 950 MHz.

(a)   (b)
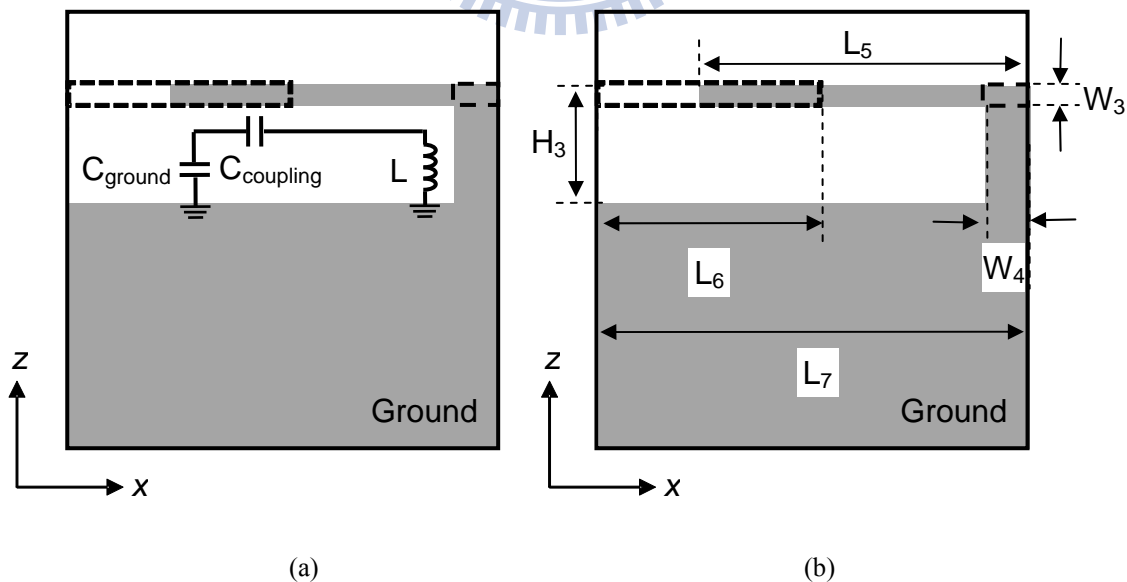
Figure 4.4: The unit cell of second 1-D EBG structure.

(a) The equivalent circuit. (b) The parameters setting.

33

The reflection phase of the second 1-D EBG structure is shown in Fig 4.5. We can notice that the bandwidth of this structure is wider than the first one because of comparatively larger inductance and smaller capacitance.
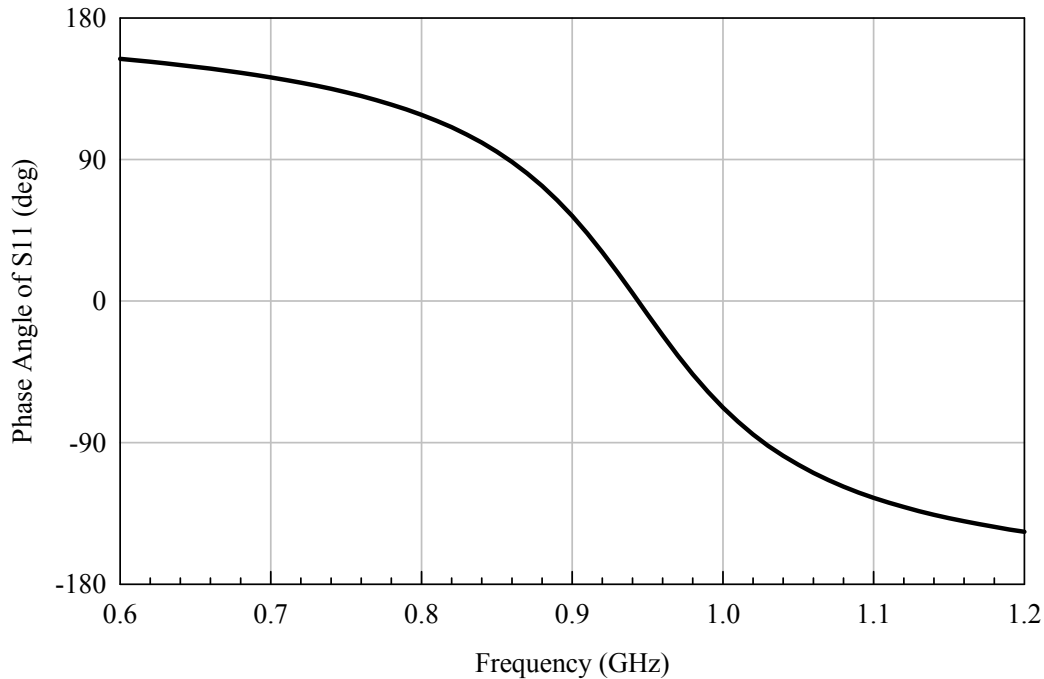
Figure 4.5: The reflection phase of second 1-D EBG structure.

4.2 DESIGN OF GROUND-PROXIMITY MONOPOLE ANTENNAS

Now we apply two proposed 1-D structures to monopole antennas respectively. We place a designed monopole antenna next to four unit cells of 1-D EBG structure on a 200mm × 300 mm ground plane, which is shown in Fig. 4.6 and Fig. 4.7. The monopole antenna is made of a 1.8 mm microstrip line and located on the center of the ground plane. To maintain the low profile advantage, the width of the monopole antenna is set to 10 mm. The physical parameters of the designed monopole antennas according to Fig. 4.6 and Fig. 4.7 are listed in Table III.
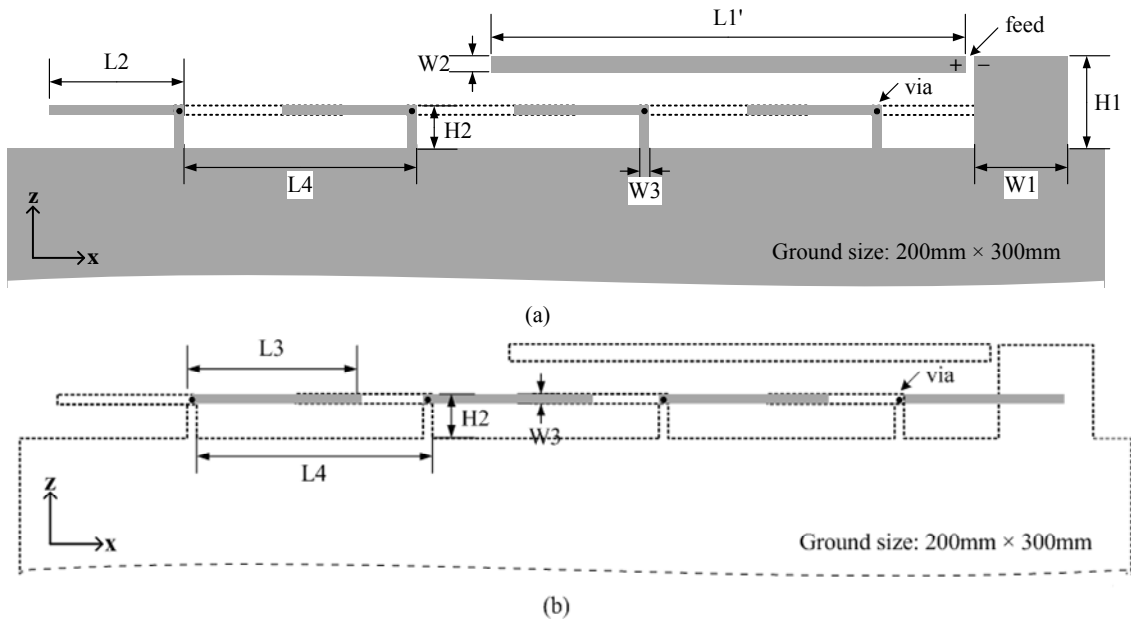
Figure 4.6: A monopole antenna designed with first 1-D EBG structure. (a) Top view. (b) Bottom view.
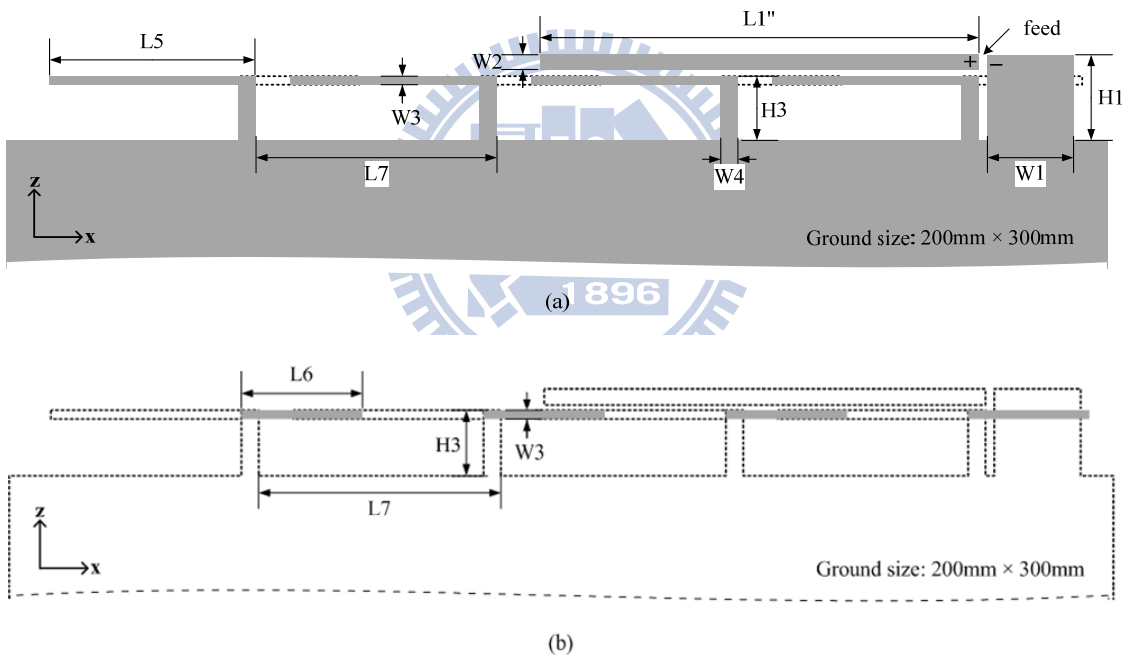
Figure 4.7: A monopole antenna designed with second 1-D EBG structure.

(a) Top view. (b) Bottom view.

TABLE III

THE PARAMETERS OF THE MONOPOLE ANTENNAS DESIGNED WITH 1-D EBG
STRUCTURES IN FIG.4.6 AND FIG 4.7

Parameters	H1	H2	H3	L1'	L1"	L2	L3	L4	L5	L6	L7	W1	W2	W3	W4
Unit:mm	10	4.6	7.8	52	48	14.5	18	25	22	14	30	10	1.8	1	2

The position that we placed 1-D EBG structure will both affect the impedance matching and the current path on the monopole antenna, so we vary the distance between feed point and the 1-D EBG structures to optimize performance of the antenna. And the lengths of the monopole antennas are also designed different slightly according to the different 1-D EBG structure for impedance matching.

This effect of 1-D EBG structures can be observed in current distribution diagram, which is shown in Fig. 4.8. The current distribution along the ground plane is weak at the resonance frequency of the applied 1-D EBG structure (840 MHz or 950 MHz). That means the image current of the monopole antenna on the ground was suppressed by 1-D EBG structure, thus the monopole antenna can radiate without being affected.

(a)
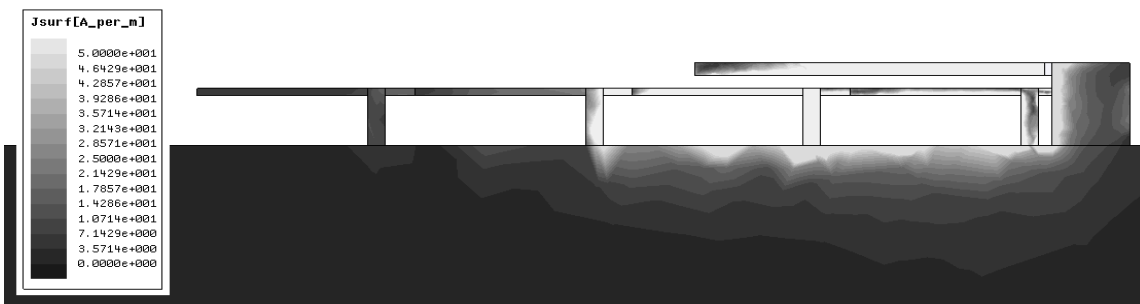
(b)

Figure 4.8: Current distributions of the proposed monopole antennas.
(a) The monopole antenna with first 1-D EBG structure at 840 MHz.
(b) The monopole antenna with second 1-D EBG structure at 950 MHz.

Moreover, most of the energy is bounded in the first two unit cells of the right side, which are the nearest to the feed point of monopole antennas. Therefore, we conclude that these two unit cells dominate the performance of 1-D EBG structure while the others are not necessary. So we can reduce the required number of unit cells and achieve a more compact antenna design. This miniaturized method will be used in next section, and the size of antenna can be reduced approximately 50 percent.

The simulated return loss of proposed monopole antennas are shown in Fig 4.9. The bandwidth of first monopole antenna is 810 MHz to 880 MHz, and the other is 911 MHz to 995 MHz. The simulated result confirms that the second 1-D EBG structure provides wider bandwidth as we mentioned in previous section. However, neither of the antenna have enough bandwidth for GSM, so these two 1-D EBG structures need to be combined to achieve wider bandwidth in next section.
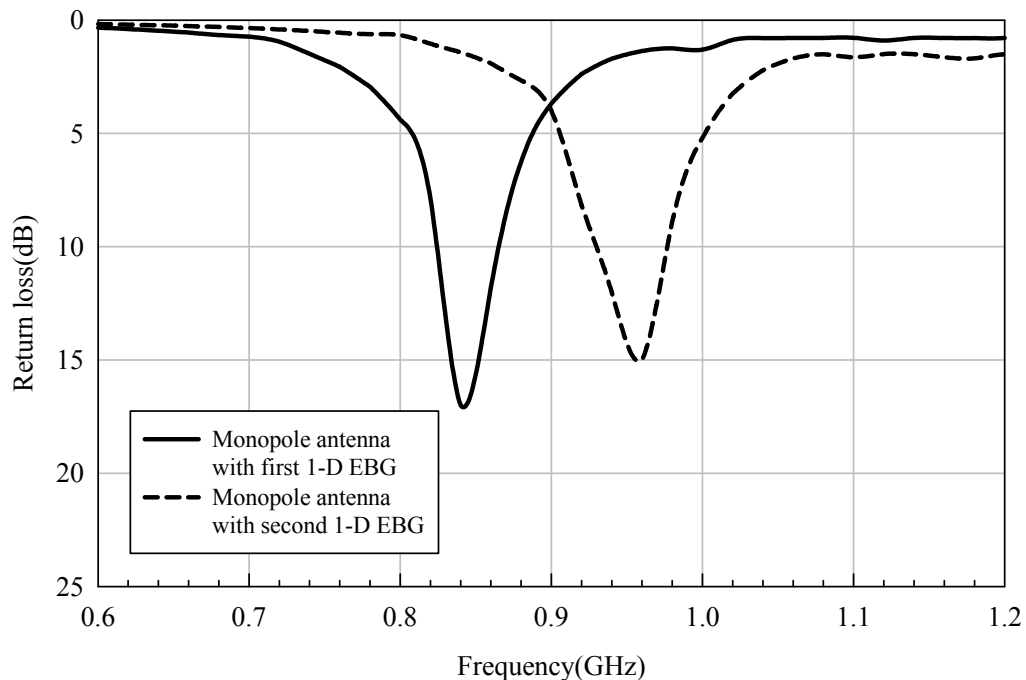
Figure 4.9: The simulated return loss of a monopole antenna with first 1D-EBG structure and a monopole antenna with second 1D-EBG structure.

4.3 DESIGN OF A PENTA-BAND GROUND-PROXIMITY MONOPOLE ANTENNA

In this section, the shortcomings mentioned in the previous section will be improved. A compact penta-band monopole antenna designed using two different kinds of 1-D EBG structures is proposed and shown in Fig. 4.10. We combined these two 1-D EBG structures together to achieve wider bandwidth in low band (824 MHz - 960 MHz), and only two unit cells of each 1-D EBG structures are used to miniaturize the total size of antenna. The total size of proposed antenna is 10 mm $\times$ 63 mm, which is applicable to laptop computers. The parameters of the designed monopole antenna according to Fig. 4.10 are listed in Table IV.
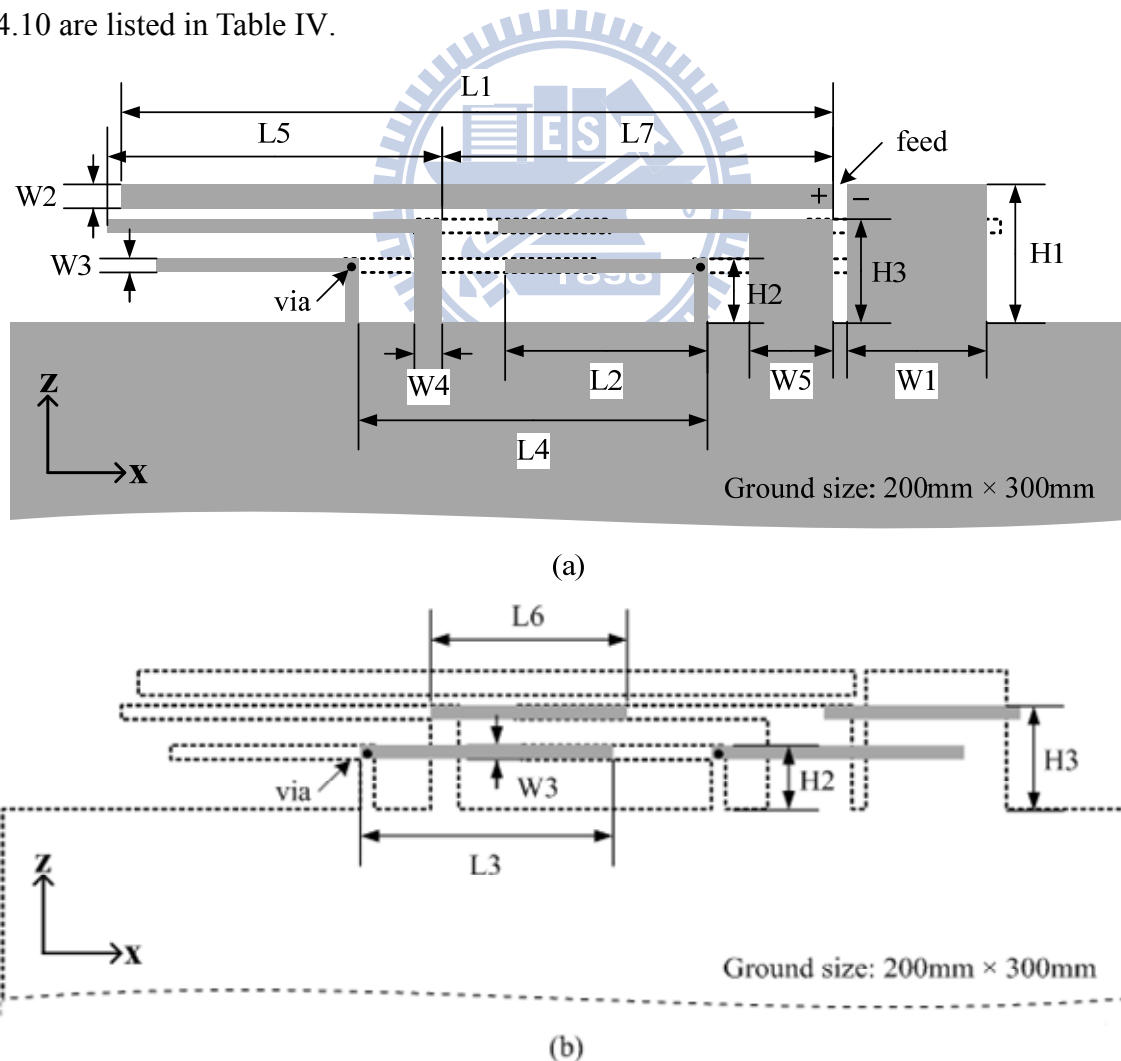
Figure 4.10: A penta-band monopole designed with 1-D EBG structures. (a) Top view. (b) Bottom view.

TABLE IV

THE PARAMETERS OF PROPOSED PENTA-BAND MONOPOLE ANTENNA

Parameters	H1	H2	H3	L1	L2	L3	L4	L5	L6	L7	W1	W2	W3	W4	W5
Unit:mm	10	4.6	7.8	51	14.5	18	25	22	14	30	10	1.8	1	2	5.8

Figure 4.11 presents the simulated return loss results of the proposed antenna. A monopole antenna with a ground plane is also simulated as a reference. When the monopole antenna is placed near to a ground plane, the radiation from the reverse image current cancels the radiation from the original monopole antenna. Thus, the return loss is only above −5.8 dB. When those two 1-D EBG structures are applied together, the return loss improves significantly. A GSM bandwidth (824 MHz - 960 MHz) is achieved in this design, and the low bandwidth ranges from 820 MHz to 1120 MHz. Furthermore, the 1-D EBG structures also radiate in high band (1710 MHz – 2170MHz), thus a penta-band antenna can be achieved after additional impedance matching.
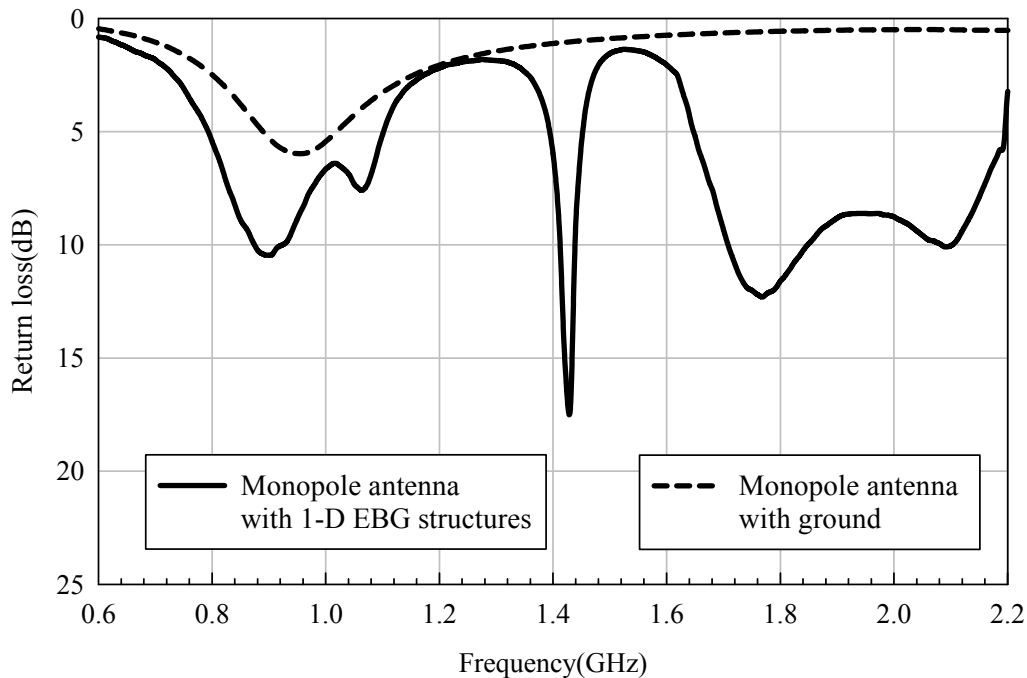
Figure 4.11: The simulated return loss of proposed penta-band monopole antenna with 1-D EBG structures, and monopole antenna with ground.

The length of monopole antenna (L_1) is slightly different to the previous applications in Fig. 4.6 and Fig 4.7. To design proper length of monopole antenna, the parameters of the 1-D EBG structures are kept the same while the monopole length is changed during the simulations. Thus, the monopole antenna will resonate at different frequencies. Since the electromagnetic property of the 1-D EBG structures are a function of frequency, its interaction with the monopole antenna is also frequency dependent. As a result, the radiation efficiency of the monopole antenna will vary with frequency. In the operational frequency band where the 1-D EBG structures provide a constructive interaction, the monopole antenna can achieve a good return loss and radiation patterns. Therefore, by observing the return loss value and radiation patterns of the monopole at different frequencies, one can find the useful operational frequency band of the 1-D EBG structures.

After combining two 1-D EBG structures, the characteristics of both structures may change unexpectedly. Therefore, we discuss the structures respectively to observe the performance of 1-D EBG structures. First, the current distribution diagram is shown in Fig. 4.12 at the resonance frequency of first 1-D EBG structure (840 MHz). Compared to Fig. 4.8(a), the current distribution is almost the same, which means the characteristics of first 1-D EBG structure remain the same at 840 MHz.

Figure 4.12: Current distributions of the proposed penta-band monopole antenna at 0.84 GHz.

Second, the current distribution diagram is shown in Fig. 4.13(a) at the resonance frequency of second 1-D EBG structure (950 MHz). Compared to Fig. 4.8(b), the current distribution is almost the same, which means the characteristics of second 1-D EBG structure remain the same at 950MHz. Furthermore, the unit cells of second 1-D EBG structure can radiate individually in high band. To achieve enough high bandwidth, one of the unit cells of second 1-D EBG structure is modified. Because of the difference between W_4 and W_5, unequal resonance frequencies in high band are created (1.8 GHz and 2.05 GHz) while the characteristics of second 1-D EBG structure in low band maintain the same. This phenomenon can be observed in current distribution diagram in Fig. 4.13. Fig. 4.13 (b) and (c) show the current distribution in high bands, which are dominated by the length and height of second 1-D EBG structure on the top side (L_5 and H_3). The resonance frequency of the left unit cell, where the strong current distribution is shown in Fig. 4.13 (b), is 1.8GHz. And the resonance frequency of the right unit cell, where the strong current distribution is shown in Fig. 4.13 (c), is 2.05GHz. The simulated return loss shown in Fig. 4.14 helps to demonstrate this property. It shows that the center frequency moves from 1.05 GHz to 1.15 GHz in low band as L_5 changes from 23 mm to 21 mm. As expected, the lowest resonance almost remains the same since the first 1-D EBG structure was not changed. The resonances in high band are both decreasing with increasing L_5, since the resonances are created by the second 1-D EBG structure in high band. Thus we can conclude that those two unit cells of second 1-D EBG can be designed to achieve the bandwidth from 1.7 GHz to 2.2 GHz, which covers the high band of penta-band application.

(a)

(b)

(c)
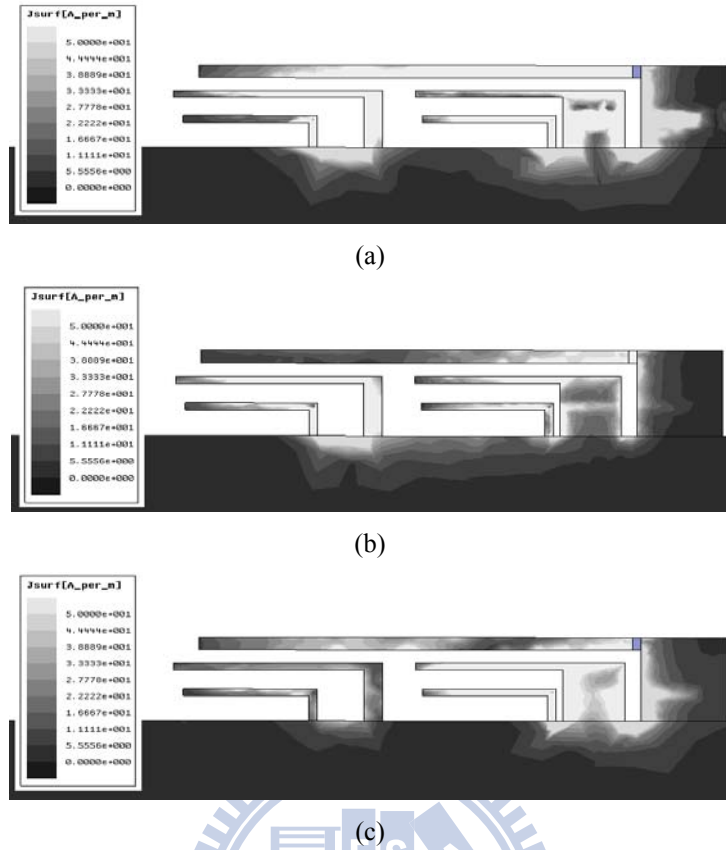
Figure 4.13: Current distributions of the proposed penta-band monopole antenna at

(a) 0.95 GHz (b) 1.8 GHz (c) 2.05 GHz.
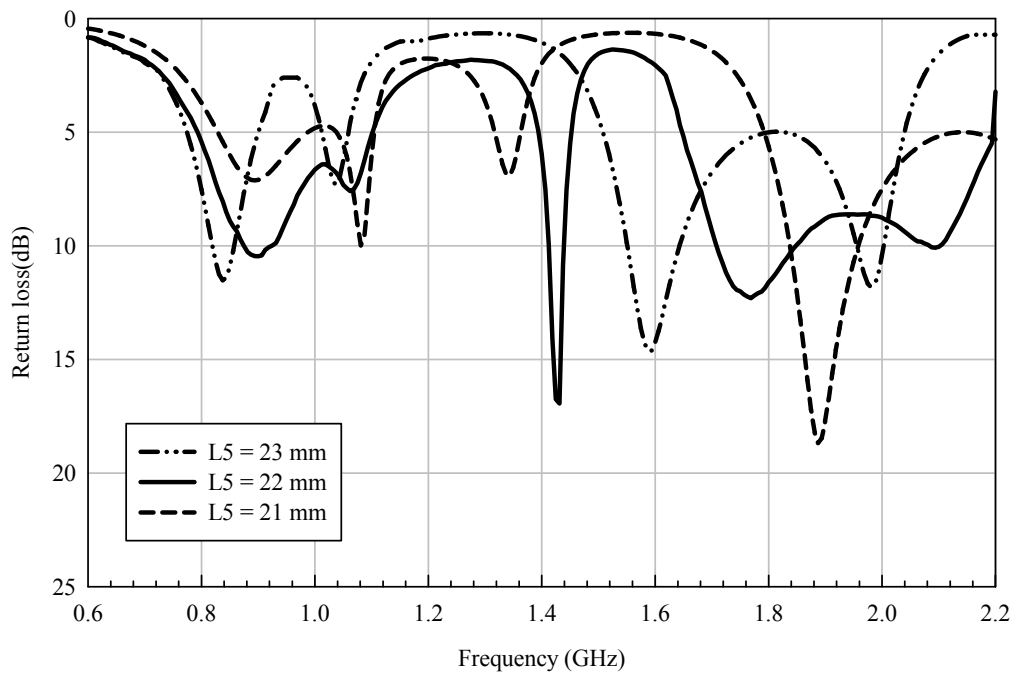
Figure 4.14: Simulated return loss for various L_5 of the proposed penta-band antenna.

4.4 EXPERIMENTAL RESULTS

The realized proposed antenna is shown in Fig.4.15.

Zoom in photo for antenna:

Ground size: 200mm × 300mm

(a)

Zoom in photo for antenna:

Ground size: 200mm × 300mm

(b)
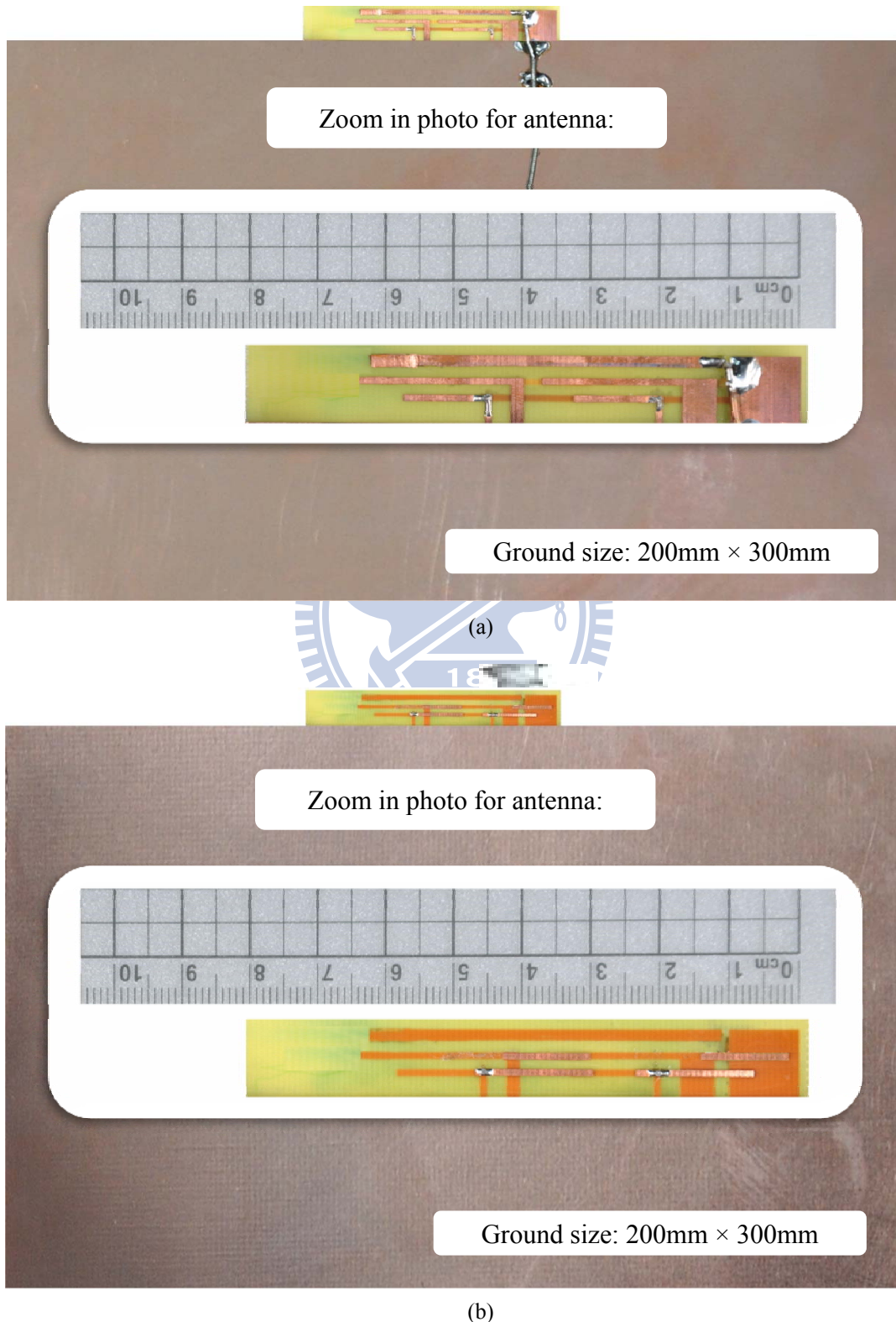
Figure 4.15: The realized proposed antenna. (a) Top view. (b) Bottom view.

In Fig. 4.16, the solid line represents the measured result and dotted line represents the simulated result of the proposed penta-band monopole antenna with 1-D EBG structures. The measured bandwidth ranges from 820 MHz to 1103 MHz and 1708 MHz to 2190 MHz with a reflectivity less than −6 dB. The measured and simulated results are generally identical, while the performance from 1900 MHz to 2100 MHz is poorer when measurement. Although the measurement is not as ideal as simulation, the bandwidth is still enough for penta-band application.
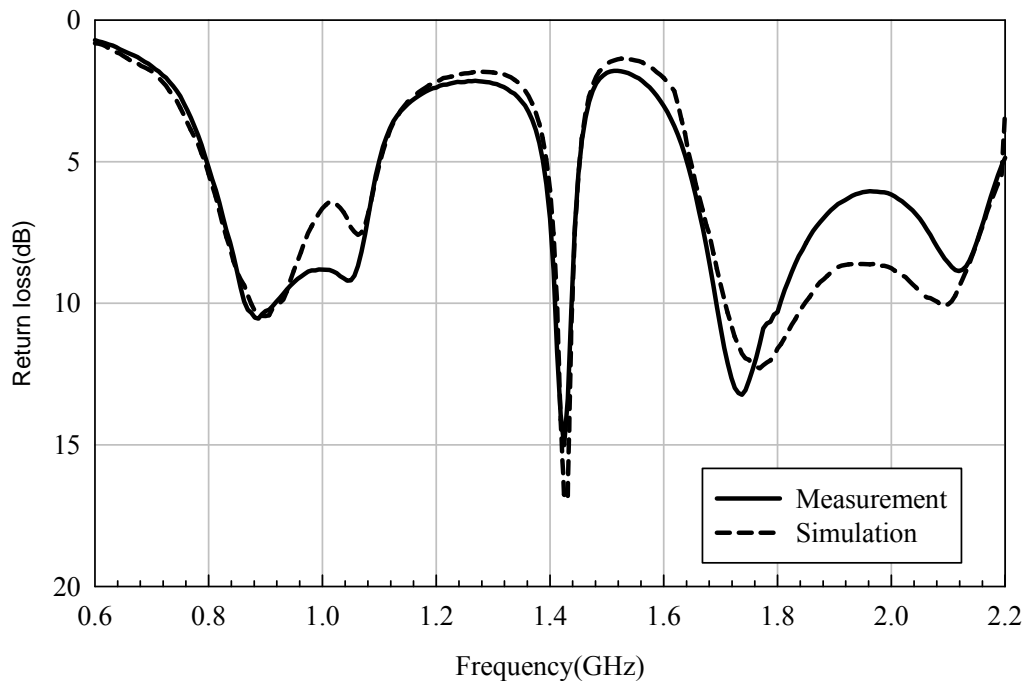
Figure 4.16: Simulated and measured results of proposed penta-band monopole antenna.

To illustrate the effect of 1-D EBG structures, we simulated and measured the radiation patterns of monopole antennas in two configurations: the proposed monopole antenna with 1-D EBG structures and a monopole antenna with ground plane. The antenna patterns are measured and simulated at 890 MHz and the *xz*, *yz*, and *xy* plane patterns are sketched in Fig. 4.17. The short distance between antenna and ground plane cause the mirror current on the ground plane opposite to the current on the antenna, and

thus eliminate each other, which leads to skew radiation pattern. By comparing the radiation pattern between the monopole antenna with and without 1-D EBG structures, the radiation pattern become more identical to theoretical radiation pattern of monopole antenna after adding 1-D EBG structures. It can be inferred from Fig. 4.17 that the radiation power is nearly omni-directional, so 1-D EBG structure is able to improve the skewed pattern of the original problem.

Phi = 0°

Phi = 90°

Theta = 90°
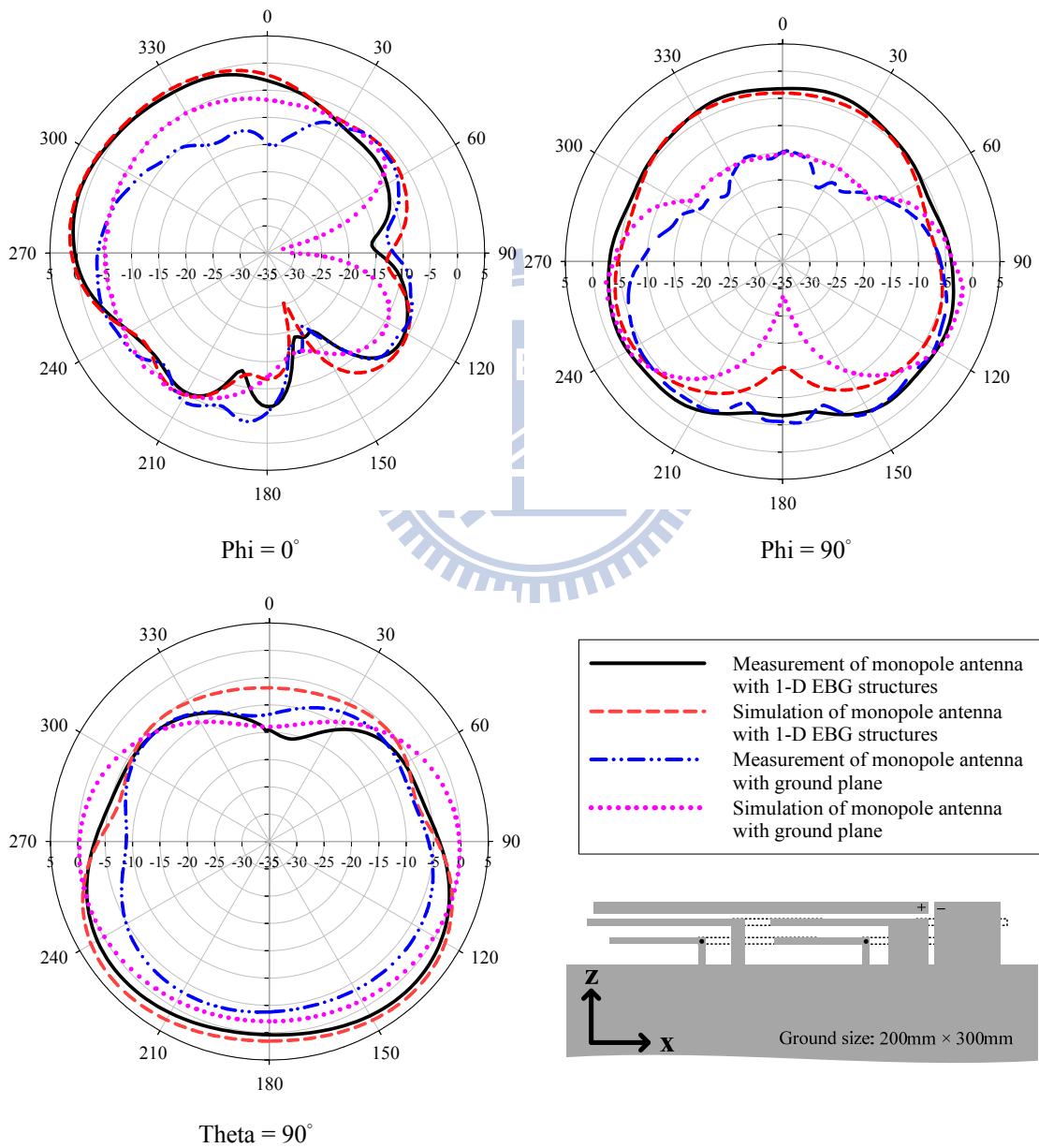
Figure 4.17: The measured and simulated patterns of monopole antenna with 1-D EBG structures and monopole antenna with ground at 890MHz.

And the xz, yz, and xy plane antenna patterns are measured at 1750 MHz, 1900 MHz, and 2150MHz in Fig.4.18 and Fig.4.19. The total radiation pattern is contributed to the direct radiation from the proposed monopole antenna and the radiation power is almost omni-directional In addition to–z direction. It is interesting to notice that the lobes on –z direction are significantly lower because of the large PEC plane placed on –z direction.

Phi = 0°

Phi = 90°

Theta = 90°
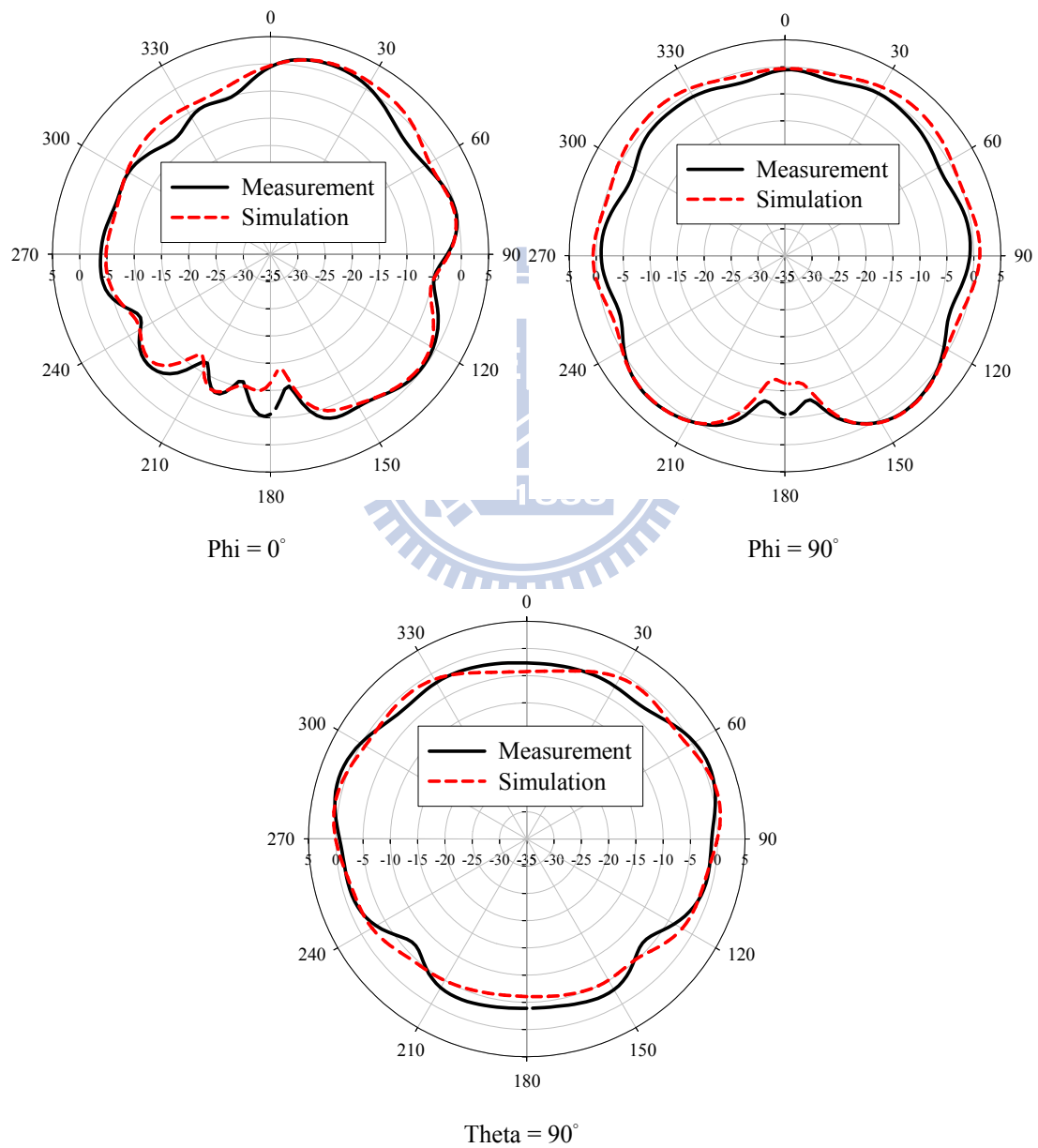
Figure 4.18: The measured and simulated patterns of proposed penta-band monopole antenna at 1750MHz.

Phi = 0°

Phi = 90°

Theta = 90°

(a)

(b)
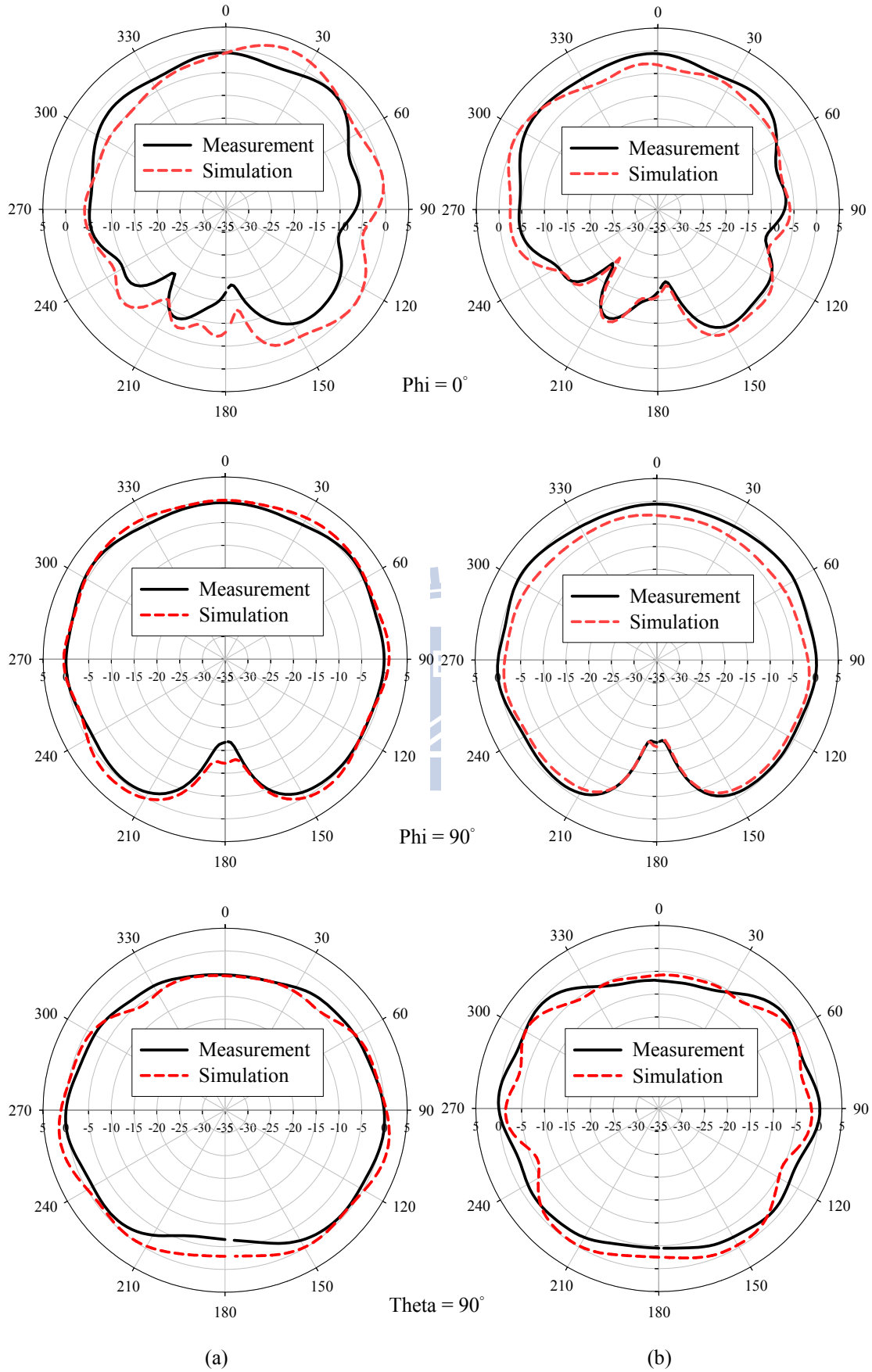
Figure 4.19:The measured and simulated patterns of proposed penta-band monopole antenna at

(a) 1900 MHz (b) 2150 MHz.

47
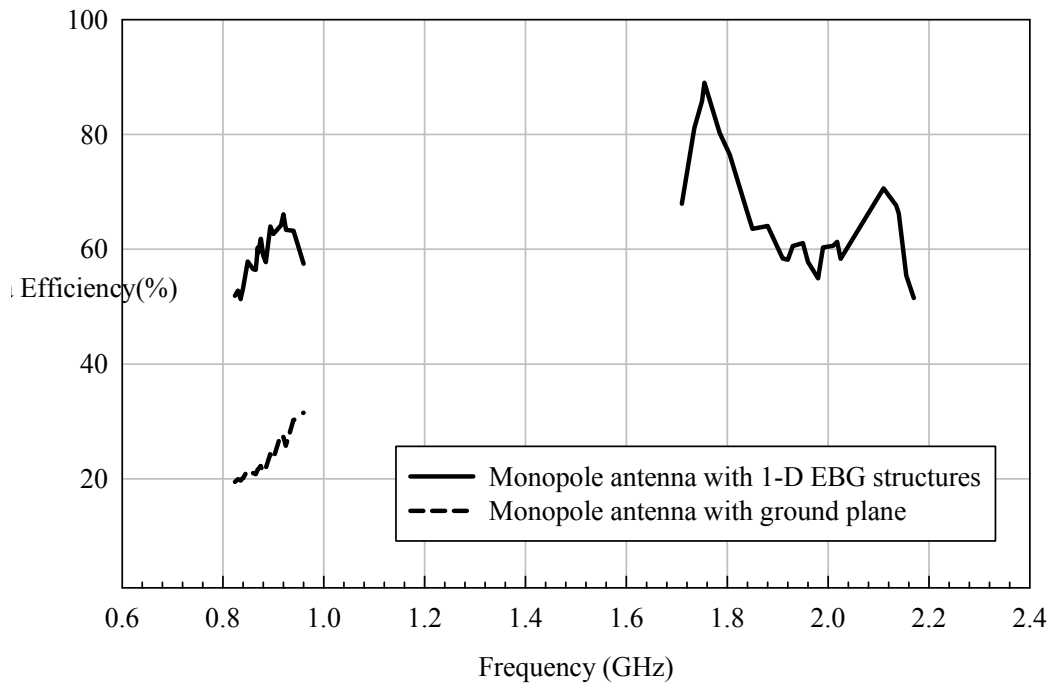
Figure 4.20: Antenna efficiency of the proposed penta-band monopole antenna with 1-D EBG structures and the monopole antenna with ground.

Fig. 4.20 indicates the antenna efficiency in the given conditions: the proposed penta-band monopole antenna with 1-D EBG structures and a monopole antenna with ground plane. The proposed penta-band monopole antenna with 1-D EBG structures has peak antenna efficiency 65% at 900 MHz. and 89.2% at 1740MHz. When the monopole antenna is placed close to the ground without 1-D EBG structures, the antenna efficiency peak drops to 31% at 960MHz. Compared to Fig. 4.14, the efficiency and the return loss of the antenna come to a great agreement. In the bandwidth of GSM (824 MHz - 960 MHz), the antenna efficiency is all above 51.3%, which has at least 32% enhancement to the case without 1-D EBG structures. And the antenna efficiency in high band (1710 MHz to 2170 MHz) is all above 51.5%, which is sufficient for commercial applications.

Chapter 5 CONCLUSIONS

The proposed 1-D EBG structure uses printed electromagnetic bandgap structure to realize parallel LC resonant circuit. To achieve the purpose of narrowing antenna size for laptop computer applications, the proposed structure reduces conventional EBG structure into planar structure. The first proposed application of 1-D EBG structure is a printed ground-proximity dipole antenna. The efficiency of proposed dipole antenna in GSM band is all above 55.6% and has at least a 10% improvement by adding 1-D EBG structure. However, the size and bandwidth of this dipole antenna need to be improved for nowadays applications. The second proposed application is a printed penta-band ground-proximity monopole antenna, which we applied two different kinds of 1-D EBG structures to achieve enough bandwidth for GSM operation. Furthermore, we adjusted the 1-D EBG structures for impedance matching and create resonance in high band, thus achieve penta-band requirement. So when applying 1-D EBG structures to antenna design, the structure can shorten the distance between antenna and ground plane and allow antennas to maintain the original radiation characteristics. And it also creates high bandwidth while the structure is well designed. The size of the antenna is reduced to 10 mm ✕ 63 mm, and the efficiency is above 51.3% in low band (824 MHz – 960 MHz) and above 51.5% in high band (1710 MHz – 2170 MHz), which is sufficient for commercial applications. Consequently, a novel type of printed penta-band antenna designed with 1-D EBG structures is proposed and is applicable to today's applications such as laptop computer, PDA, mobile phone antennas.

REFERENCE

[1] Wikipedia. Available: http://en.wikipedia.org/wiki/WWAN

[2] K.R. Boyle, P.G. Steeneken, "A Five-Band Reconfigurable PIFA for Mobile Phones," *Antennas and Propagation*, vol. 55, Issue 11, pp. 3300-3309, Nov. 2007.

[3] R.F.J. Broas , D.F. Sievenpiper, and E. Yablonovitch, "A High-Impedance Ground Plane Applied to a Cellphone Handset Geometry," *Microw. Theory and Techniques*, vol. 49, Issue 7, no. 6, pp. 1262-1265, August. 2002.

[4] M.F. Abedin, M.Z. Azad, and M. Ali, "Wideband Smaller Unit-Cell Planar EBG Structures and Their Application," *Antennas and Propagation*, vol. 56, Issue 3, pp. 903-908, March 2008.

[5] H. D. Yang, N. G. Alexopoulos, and E. Yablonovitch, "Photonic band-gap materials for high-gain printed circuit antennas," *IEEE Trans. Antennas Propag.*, vol. 45, no. 1, pp. 185–187, Jan. 1997.

[6] R. Coccioli, F. R. Yang, K. P. Ma, and T. Itoh, "Aperture-coupled patch antenna on UC-PBG substrate," *IEEE Trans. Microw. Theory Tech.*, vol. 47, pp. 2123–2130, Nov. 1999.

[7] M. Rahman and M. Stuchly, "Wide-band microstrip patch antenna with planar PBG structure," n *Proc. IEEE AP-S Int. Symp. Dig.*, Jul. 2001,vol. 2, pp. 486–489.

[8] S. Sharma and L. Shafai, "Enhanced performance of an aperture-coupled rectangular microstrip antenna on a simplified uniplanar compact photonic bandgap (UCPBG) structure," in *Proc. IEEE AP-S Int. Symp.Dig.*, Jul. 2001, vol. 2, pp. 498–501.

[9] J. S. Colburn and Y. Rahmat-Samii, "Patch antennas on externally perforated high dielectric constant substrates," *IEEE Trans. Antennas Propag.*, vol. 47, pp. 1785–1794, Dec. 1999.

[10] F. Yang and Y. Rahmat-Samii, "Mutual coupling reduction of microstrip antennas using electromagnetic band-gap structure," in *Proc. IEEE AP-S Int. Symp. Dig.*, Jul. 2001, vol. 2, pp. 478–481.

[11] R. Gonzalo, P. de Maagt, and M. Sorolla, "Enhanced patch-antenna performance by suppressing surface waves using photonic-bandgap substrates," *IEEE Trans. Microw. Theory Tech.*, vol. 47, no. 11, pp.2131–2138, Nov. 1999.

[12] Y. J. Park, A. Herschlein, and W. Wiesbeck, "A photonic bandgap (PBG) structure for guiding and suppressing surface waves in millimeter-wave antennas," *IEEE Trans. Microw. Theory Tech.*, vol. 49, no. 10, pp. 1854–1859, Oct. 2001.

[13] F. Yang and Y. Rahmat-Samii, "Microstrip antennas integrated with electromagnetic band-gap (EBG) structures: A low mutual coupling design for array applications," *IEEE Trans. Antennas Propag.*, vol. 51, pp. 2939–2949, Oct. 2003.

[14] M. F. Abedin and M. Ali, "Effects of a smaller unit cell planar EBG structure on the mutual coupling of a printed dipole array," *IEEE Antennas Wireless Propag. Lett.*, vol. 4, pp. 274–276, 2005.

[15] F. Yang and Y. Rahmat-Samii, "A low profile circularly polarized curl antenna over electromagnetic band-gap (EBG) surface," *Microw. Opt. Tech. Lett.*, vol. 31, no. 4, pp. 478–481, Nov. 2001.

[16] F. Yang and Y. Rahmat-Samii, "Reflection phase characterizations of the EBG ground plane for low profile wire antenna applications," *IEEE Trans. Antennas Propag.*, vol. 51, no. 10, pp. 2691–2703, Oct. 2003.

[17] M. F. Abedin and M. Ali, "Effects of EBG reflection phase profiles on the input impedance and bandwidth of ultra-thin directional dipoles," *IEEE Trans. Antennas Propag.*, vol. 53, no. 11, pp. 3664–3672, Nov. 2005.

[18] M. F. Abedin and M. Ali, "A low profile dipole antenna backed by a planar EBG structure," *Proc. IEEE Int. Workshop on Antenna Tech., Small Antennas and Novel Metamaterials*, Mar. 6–8, 2006, pp. 13–16.

[19] Z. Li and Y. Rahmat-Samii, "PBG, PMC and PEC ground planes: A case study of dipole antennas," *Proc. IEEE AP-S Int. Symp. Dig.*, Jul. 2000, vol. 2, pp. 674–677.

[20] D. Sievenpiper, L. Zhang, R. F. J. Broas, N. G. Alexopolus, and E. Yablonovitch, "High-impedance electromagnetic surfaces with a forbidden frequency band," *IEEE Trans. Microw. Theory Tech.*, vol. 47, pp.2059–2074, Mar. 1999.

[21] A. S. Barlevy and Y. Rahmat-Samii, "Characterization of electromagnetic band-gaps composed of multiple periodic tripods with interconnecting vias: concept analysis, and design," *IEEE Trans. Antennas Propag.*, vol. 49, pp.242–353, Mar. 2001.

[22] F.-R.Yang, K.-P. Ma,Y. Qian, and T. Itoh, "A uniplanar compact photonic-bandgap (UC-PBG) structure and its applications for microwave circuit," *IEEE Trans. Microwave Theory Tech.*, vol. 47, pp.1509–1514, Nov. 1999.

[23] V. Radisic, Y. Qian, R. Coccioli, and T. Itoh, "Novel 2-D photonic bandgap structure for microstrip lines," *IEEE Microw. and Guided Wave Lett.*, vol. 8, no. 2, pp. 69–71, 1998.

[24] S. Clavijo, R. E. Diaz, and W. E. McKinzie, "Design methodology for Sievenpiper highimpedance surfaces: an artificial magnetic conductor for positive gain electrically small antennas," *IEEE Trans. Antennas Propag.*, vol. 51, no. 10, pp. 2678–2690, Jul. 2003.

[25] H. Nakano, K. Hitosugi, N. Tatsuzawa, D. Togashi, H. Mimaki, and J. Yamauchi, "Effects on the radiation characteristics of using a corrugated reflector with a helical antenna and an electromagnetic band-gap reflector with a spiral antenna," *IEEE Trans. Antennas Propag.*, vol. 53, no. 1, pp.191–199, Oct. 2005.

[26] M. Rahman and M. A. Stuchly, "Transmission line–periodic circuit representation of planar microwave photonic bandgap structures," *Microw. Opt. Tech. Lett.*, vol. 30, no. 1, pp. 15–19, Dec. 2001.

[27] D. F. Sievenpiper, *High Impedance electromagnetic surfaces*, Ph.D. dissertation, Electrical Engineering Department, University of California, Los Angeles, 1999.

[28] G. V. Eleftheriades and K. G. Balmain, *Negative Refraction Metamaterials: Fundamental Principles and Applications*, Wiley-IEEE Press, 2005.

[29] High Frequency Structure Simulator (HFSS). Ansoft Corporation, Pittsburgh, PA, 2001.